The TREND IN ENGINEERING

at the University of Washington

In this issue:

A NEUTRON ABSORPTIOMETER FOR THE ON-STREAM ANALYSIS OF BORON

WATER DISINFECTION AT A NATURAL SWIMMING BEACH

ON THE BRITTLE FRACTURE OF STRUCTURES

LUNAR TIDAL VARIATIONS IN THE IONOSPHERIC LAYERS

THE IMPLICATIONS OF ISENTROPIC NOZZLE FLOW FOR A PERFECT GAS

April, 1960

Published quarterly

by

THE ENGINEERING EXPERIMENT STATION

THE ENGINEERING EXPERIMENT STATION of the University of Washington, which was established in December, 1917, performs a three-fold function:

1) It stimulates, promotes, and coordinates investigations and research in all fields of engineering.
2) It publishes results of significant research achievements.
3) It provides opportunities through Graduate Research Assistantships for engineering students to extend their professional education while pursuing a course of study leading to the M.S. or Ph.D. degree.

For administrative purposes the work of the Station is organized under six divisions. All research is carried on in the various academic departments of the College of Engineering under the supervision of the department faculties.

The control of the Station is vested in the Station Board consisting of the Dean of the College of Engineering as chairman, the Director of the Station, and the executive officers of the academic departments.

The Station offers a substantial number of Research Assistantships to highly qualified graduate students who are assigned to the academic departments. Results of major investigations are published by the Station in the form of bulletins and reports. Current research findings, as well as listings of sponsored research projects, appear in the quarterly journal, *The Trend in Engineering at the University of Washington.* Reprints of articles by members of the engineering faculty and graduate students published in recognized technical journals are also issued by the Station.

Applications for Assistantships, requests for copies of the publications and inquiries for information on engineering and industrial research problems should be addressed to the Director, Engineering Experiment Station, University of Washington, Seattle 5.

April, 1960 The TREND

IN ENGINEERING

Vol. 12 No. 2

at the University of Washington

Published quarterly in January, April, July and October, by the Engineering Experiment Station at the University of Washington to reflect the current highlights of its accomplishments and to report progress in its program of investigation and research.

ENGINEERING EXPERIMENT STATION BOARD

Chairman..... Harold E. Wessman
Dean of the College of Engineering

Director of the Engineering Experiment Station..... F. Burt Farquharson

DEPARTMENT REPRESENTATIVES

Aeronautical Engineering..... H. C. Martin
Chemical Engineering..... R. W. Moulton
Civil Engineering..... R. B. Van Horn
Electrical Engineering..... A. V. Eastman
Mechanical Engineering..... B. T. McMinn
Mineral Engineering..... D. A. Pifer

PUBLICATION COMMITTEE

F. B. Farquharson W. R. Hill
R. G. Hennes B. D. Mills, Jr.

Editor..... H. Harold Kelley

PUBLICATION OFFICE

127 More Hall
University of Washington
Seattle 5, Washington

Entered as second-class matter March 7, 1949, at the post office at Seattle, Washington, under the Act of August 24, 1912.

CONTENTS

A Neutron Absorptiometer for the On-Stream Analysis of Boron *Carroll L. Pleasance* 2

Water Disinfection at a Natural Swimming Beach *Robert O. Sylvester* 5

On the Brittle Fracture of Structures *Paul C. Paris, William E. Anderson* 11

Lunar Tidal Variations in the Ionospheric Layers *N. Narayana Rao, H. Myron Swarm* 15

The Implications of Isentropic Nozzle Flow for a Perfect Gas *Charles P. Costello, William B. Nordquist* 23

Engineering Research Dividends 28

A Study of Fuel Consumption and Travel Time Characteristics of Diesel Powered Vehicles *D. L. Crumbley*

Boundary Layer Transition in Natural Convection *J. R. Larson*

The Semi-Diurnal Lunar Variations of Ionospheric Layers *N. N. Rao*

The Use of Metallic Thermocouples as Heat Engines *R. L. Straley*

Notes and Comments 29

Engineers in the News

New Projects

A Neutron Absorptiometer for the On-Stream Analysis of Boron

CARROLL L. PLEASANCE
*Process Control Development Engineer**

C. L. Pleasance

K. B. Bengtson

INTRODUCTORY

Carroll L. Pleasance graduated from the University of Washington in 1951 with a B.S. Degree in Electrical Engineering. Since graduation he has been employed by the General Electric Company at its Hanford Atomic Products Operation. Since 1954 he has worked on the development and application of control instrumentation for chemical process plants. While working in Richland, he has been enrolled at the University of Washington Center for Graduate Study at Hanford, where he is working toward the degree of Master of Science in Engineering with a Nuclear Option.

The paper presented here marks an occasion because Mr. Pleasance is a candidate for one of the first degrees to be obtained through academic work mostly done at Hanford and because it is the first work by a Hanford student to appear in *Trend*. Mr. Pleasance's paper deals with research work he performed as part of his assigned professional duties at the Hanford project; he intends to submit a more detailed report of this experimental work in fulfillment of the thesis requirement for the M.S. degree that he expects to receive this spring.—KERMIT B. BENGTSON, *Director, University of Washington Center for Graduate Study at Hanford.*

Hanford Atomic Products Operation has undertaken development studies for reprocessing power-reactor fuels. This program involves the chemical extraction and recovery of valuable nuclear materials from the fuel of privately owned power reactors. These fuels contain higher concentrations of Uranium-235 than is routinely processed in the existing separations plant; and the presence of this Uranium-235 in solution may create high neutron fluxes in process vessels. The possibility exists of producing critical mass in vessels that are not critically safe. Solution concentration control is used as a primary means of criticality control. However, boron is to be added to some process solutions to increase the thermal neutron cross section: this will reduce the neutron flux and avoid the possibility of an uncontrolled critical reaction. Thus a boron addition will afford an extra margin of nuclear safety during processing of power-reactor fuels.

An on-stream analyzer is needed to determine whether process solutions contain sufficient boron to assure the extra safety factor. This paper describes such an analyzer, an absorptiometer. It was designed for installation at a particular point in the separations plant. Shown in Fig. 1 is the physical arrangement of the operating gallery, pipe gallery, and process cell. In the operating gallery, cold chemical solutions are prepared in chemical make-up tanks prior to addition to the process. These solutions flow by gravity from the operating gallery through the pipe gallery to the process cell. The analyzer will be installed in the pipe gallery; readout will be done in the operating gallery.

The solutions that pass through the analyzer are 60% nitric acid, 50% sodium hydroxide, 38% sodium nitrate, and water. Each of these solutions contains approximately 1 g per liter of boron in the form of boric acid. Owing to the large volumes of solution that must be handled, the analyzer should allow a flow of at least 50 gal per minute to the process with a full make-up tank. The instrument apparently did not need to be more precise than $\pm 10\%$, the idea being that when it detected too low a boron concentration the boron would probably be completely absent from the solution. The instrument must respond and indicate a lack of boron in solution in less than 15 sec. This installation is to be a prototype for plant evaluation; therefore only alarm circuitry, such as indicating lights, is necessary. Control circuitry may be added when the monitor has demonstrated satisfactory performance.

Stromatt surveyed the literature on methods of

* The author works for Hanford Laboratories, General Electric Company, Richland, Washington, where the work described in this paper was performed under contract No. AT-(45-1)-1350 for the U.S. Atomic Energy Commission.

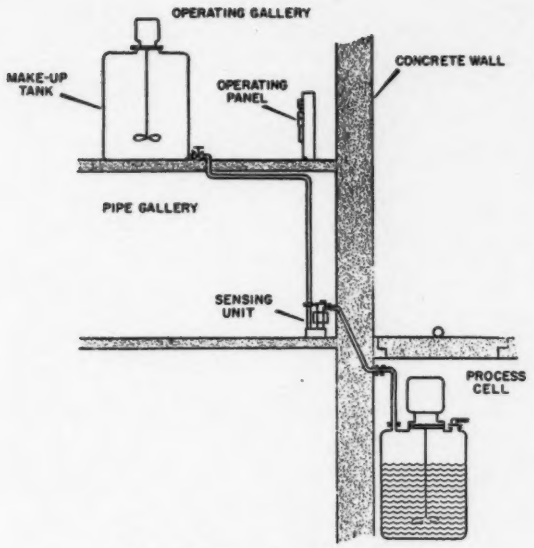

FIG. 1. BUILDING ARRANGEMENT

analysis for boron.[1] His study reveals that boron may be analyzed by colorimetric, volumetric, spectrographic, flame photometric, polarographic, polarimetric, and neutron-absorption methods. Most of these methods are not readily adaptable to rapid on-stream analysis of boron since they generally measure total boron rather than selectively analyze for the neutron-absorbing isotope boron-10. The thermal neutron cross section of the solution is the specific property that needs to be determined. Since neutron-absorption techniques measure precisely this property, the development of a neutron absorptiometer was begun.

The Sensing Unit

A coaxial arrangement of the sensing unit was planned as shown in Fig. 2. DeFord and Braman found that such a configuration produces the best counting geometry.[2] The sensing unit consists of three parts—a Source and Moderator, a Sensing Cell, and a Seal Pot.

Source and Moderator. The source used in the monitor is a plutonium-beryllium neutron source emitting 1.5 x 10^5 neutrons per sec. The source produces neutrons by an alpha → neutron (α, n) reaction, the alpha particle being produced from the plutonium decay:

$$_4Be^9 + {}_2He^4 \rightarrow {}_6C^{12} + {}_0n^1 + Q.$$

The energy associated with the neutron is usually greater than 5 mev; so this is called a "fast" neutron. To be utilized for measurement of boron concentration, the neutrons must be slowed to "thermal" energies (less than 0.05 ev) to permit capture by the boron in the solution undergoing analysis. This slowing down is accomplished by placing a paraffin moderator around the source. The fast neutrons enter the moderator and undergo elastic collisions with hydrogen and carbon atoms. This both scatters the neutrons throughout the moderator and slows them to thermal energy levels. Thus there is a three-dimensional distribution of thermal neutrons traveling throughout the moderator. A certain percentage of these neutrons travel through the sensing cell and are measured by the neutron detector tube. As the thermal neutron cross section of the solution in the sensing cell increases, the counting rate of the detector decreases; therefore the counting rate is inversely proportional to the thermal neutron cross section of the solution.

Sensing Cell. Once the counting geometry of a particular configuration of source, moderator, and sensing cell has been determined, the calibration curve may be approximated by calculating the change in macroscopic cross section as the solution concentration in the sensing cell is varied. For a high sensitivity to low concentrations of boron, the sensing cell and moderator housing must be fabricated in such a manner and of such materials as to minimize the absorption cross section. Experimentally it was determined that a thin-walled stainless-steel cell with a

(Continued on page 31)

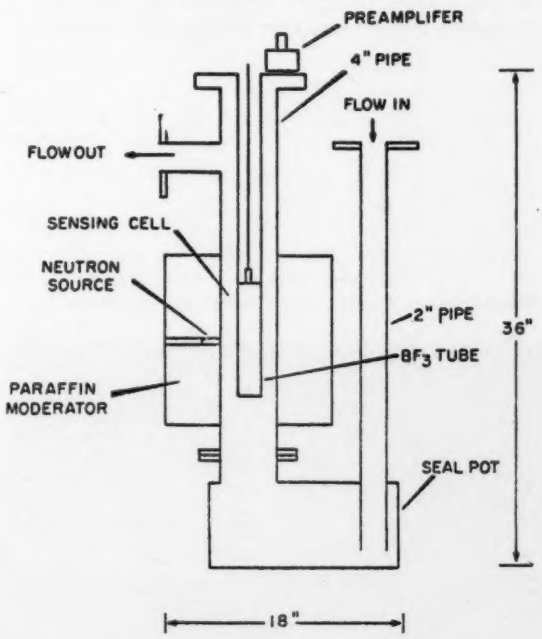

FIG. 2. SKETCH OF NEUTRON ABSORPTIOMETER

FIG. 1. MAP SHOWING GREEN LAKE (LEFT CENTER) AND VICINITY

FIG. 2. MAP SHOWING RECREATIONAL USE OF GREEN LAKE

FIG. 3. WEST GREEN LAKE BEACH (COURTESY SEATTLE P.I.)

FIG. 4. EAST GREEN LAKE BEACH (COURTESY SEATTLE P.I.)

Water Disinfection at a Natural Swimming Beach

ROBERT O. SYLVESTER
Professor of Sanitary Engineering

R. O. Sylvester

In February, 1959, the University of Washington, through its Department of Civil Engineering and at the request of the City of Seattle, entered into a contract with the Seattle Park Commissioners for a study of Green Lake that would result in recommendations for rehabilitation of the Lake. The Lake has a surface area of 256 acres, a shoreline of 2.9 miles, and an average depth of 12.5 feet. It contains some 1088 million gallons of water. It is surrounded by a thickly populated residential area in the north-central portion of Seattle. Green Lake lies on the margin of the University District.

Because of its location and character, Green Lake has a present and potential recreational usage that is not excelled by any other lake of its size in the United States (see Figs. 1 and 2). The full realization of this potential has been jeopardized by heavy algal blooms during the swimming season, by "swimmers' itch," sewage backflow into the lake, and by the maturation of the Lake to the stage of rapid shoaling, with the appearance of swampy characteristics about its shoreline. During the period of 1953-57, the yearly average number of swimmers was about 350,000. Green Lake was closed to swimming during a portion of the 1958 season because relatively high coliform bacterial densities were observed in the Lake water and because the North Trunk Sewer had previously collapsed and backflowed into it.

A portion of the contractual agreement for the overall Lake study called for an immediate study of what interim measures might be taken to improve water quality at the two Green Lake bathing beaches in time for the 1959 season. This article summarizes the report on these interim measures,[1] including the operating data for the 1959 season. The report on the general lake study, with recommendations for a program of lake rehabilitation, was submitted to the City of Seattle in February, 1960.[2]

Physical Characteristics of Beach Areas

Of the two swimming beaches on Green Lake, one on the west shore and the other on the east, the West Beach has the best facilities and the most attractive surroundings (Fig. 3). Each beach has a supervised frontage of 380 ft and an offshore limit of 145 to 200 ft, giving each a water area of about 72,000 sq ft. The water at the West Beach extends to a depth of 14 ft, and the water volume in the beach area is 5.2 million gal; the East Beach (Fig. 4) extends to 20 ft and has a water volume of 6.3 million gal. Most of the West Beach has a sand and gravel bottom except for the very outer portion, where mud depths range from 3 to 13 ft. At the East Beach, the entire bottom is mud except for the central portion and the shallow-water areas, which are sand. Mud depths range from 7 to 13.5 ft throughout the swimming portion of the beach area.

Water currents were measured at both beaches by using drogues and dye. Light winds produced a water movement of 150 to 220 ft per hr in the upper 6 ft, and moderate winds produced velocities of 230 to 300 ft per hr. On a calm morning, several hours after a moderate wind had been blowing, erratic water movement still persisted with velocities of 90 to 125 ft per hr. The average surface wind velocities and direction at the Seattle Weather Station during the swimming season (for 20-yr and 38-yr averages) are as follows:

	June	*July*	*August*	*September*
Avg wind velocity, mph	4.2	3.9	3.7	3.9
Predominant direction	S	N	N	S

Thus in summer, with light northerly or southerly winds, we could expect that the water in the swimming areas would be exchanged by surrounding lake water in from two to four hours. During periods of calm weather (with no appreciable wind for several days) the water in the bathing area would experience only a slight exchange with the surrounding water. These periods of prolonged calm are infrequent.

Schemes of Water-Quality Improvement

Any water-treatment measures that might be used to improve the water quality for swimming in Green Lake during the 1959 season needed to have public acceptance of their reliability at the outset; be capable of simple operation; be limited in their effect on the Lake; be relatively inexpensive, since they might not fit into a program of long-range lake improvement; be suitable for easy construction, to permit their completion in time for the swimming season; and, above all, needed to eliminate the health

hazard that has been associated with swimming in Green Lake.

A number of schemes that might have resulted in improved water quality at the swimming beaches were investigated, including water treatment with a recirculation system of lake water, the addition of copper sulfate for algae control to improve the water's appearance and the functioning of a purification system, diking off the swimming areas, admission of city water to the beaches, and chlorinating the lake water at the beaches.

The installation of a system at the bathing beaches to recirculate lake water through a chemical precipitation plant, with chlorination to follow, was not practicable because of its high cost and because the water opposite a beach is being continually exchanged with outer lake water, so that treatment of the entire lake becomes necessary. A water-treatment plant capable of treating the average water supply for a city of 20,000 persons would be required just to exchange all the lake water through the plant but once a year. Such a plant would also have no appreciable effect on the overall algal problem of the lake unless large quantities of lime and alum were added to precipitate phosphorus.

An alternative remedy would be to construct a dike around each of the two bathing beaches, dredge the bottom sediments, and replace them with sand. A dike constructed of a nonorganic, silt-free mixture of sand and gravel would require frequent repair unless protected with concrete or similar walls. Recirculation of this contained water through a filtration plant would be required, since dilution and dispersion of this diked-in water with outside lake water would now be precluded. If these diked-in areas were to contain as much water as is now available at the beaches (five to six million gal each), and if State Health Department requirements for water exchange and filtration rates were observed (exchange every 6 hr with a filtration rate of 3 gpm per sq ft of sand in a pressure filter), quite an array of equipment would be required at each beach: two 7,000-gpm recirculation pumps; one alum and one lime feeder, each capable of feeding 2500 lb per 24 hr; one chlorinator with a feeding rate of 250 lb per 24 hr; and eighteen 10- by 25-ft pressure filters. The expense of constructing and operating this system to accommodate the same number of bathers now served at the natural beaches was not feasible. If the water volumes were reduced at these beaches to about half their present volumes, the cost would still be very high; and the remainder of Green Lake would be no better than before for the many other recreational uses.

The best scheme for meeting the requirements appeared to be a system that would diffuse chlorinated water into the swimming areas rapidly enough to overcome the chlorine demand of new lake water constantly being brought into the beach area by wind-driven currents. Treatment at the West Green Lake beach was recommended over the one on the east shore because the beach bottom, water depths, and water currents are more suitable for proper functioning of a disinfection system and because the East Green Lake area has, besides the beach, a swimming pool, baseball field, and boat-rental facilities. Another recommendation was that the East Green Lake beach be opened for swimming during the 1959 season, to be closed only if there was evidence of undesirable fecal pollution from human sources. Much valuable data on the effectiveness of the treatment proposed and on the epidemiological relationship[3] between the two beaches could be obtained if both beaches were kept open.

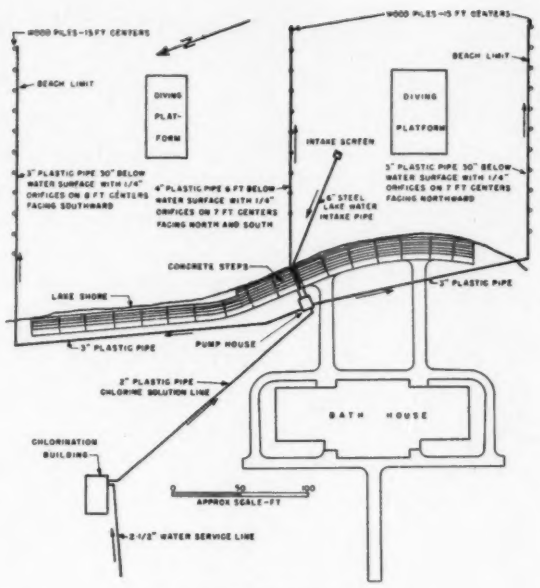
WOOD PILES—15 FT CENTERS
BEACH LIMIT
DIVING PLATFORM
INTAKE SCREEN
3" PLASTIC PIPE 30" BELOW WATER SURFACE WITH 1/4" ORIFICES ON 8 FT CENTERS FACING SOUTHWARD
4" PLASTIC PIPE 6 FT BELOW WATER SURFACE WITH 1/4" ORIFICES ON 7 FT CENTERS FACING NORTH AND SOUTH
6" STEEL LAKE WATER INTAKE PIPE
3" PLASTIC PIPE 30" BELOW WATER SURFACE WITH 1/4" ORIFICES ON 7 FT CENTERS FACING NORTHWARD
CONCRETE STEPS
LAKE SHORE
3" PLASTIC PIPE
PUMP HOUSE
2" PLASTIC PIPE CHLORINE SOLUTION LINE
BATH HOUSE
CHLORINATION BUILDING
APPROX SCALE—FT
2-1/2" WATER SERVICE LINE

FIG. 5. SCHEME OF DISINFECTION

Disinfection of natural bathing areas was known to have been used at the following locations, most of which are ponds having little water motion:

Blue Lake near Portland, Ore.
Wallace Lake near Cleveland, Ohio.
Watchung Lake, Plainfield, N.J.
Skytop Lodge, Barret Township, Pa.
Sons of Poland Camp, Inc., Morris County, N.J.
Field's Grove Pool, Nashua, N.H.
Community Park Pool, Woodbury, N.Y.
Fountain Spring Lake, Wanaque, N.J.
Riverdale Pool, Riverdale, N.J.
Paramus Beach, Paramus, N.J.

Required Chlorine Dosages

The quantities of chlorine required to kill bacteria and to maintain a chlorine residual of at least 0.2 ppm in the lake water were determined by pilot-plant experiments with water diffusers at the Aqua Theater Pool (another Green Lake recreational attraction) and by laboratory experiment, in which lake water was "doctored" in an attempt to simulate the extreme conditions of water quality that might be found at a bathing beach with a crowded bathing schedule and with a heavy sediment and algal load. (Data were not available on water-quality constituents present at a Green Lake bathing beach during a summer swimming season). The results of these laboratory and field tests, together with those obtained from the Seattle Water Department, are given below. These values gave a rate of chlorine feed ranging from 420 to 1670 lb per 24 hr when applied to the West Beach requirements. Assuming a 9-hr day of chlorination, the actual amount of chlorine added to the water at the West Green Lake bathing area would range from 160 to 320 lb per day. The following tabulation shows the dosage required to give a chlorine residual of 0.2 ppm within the stated periods of time:

Detention Times (hr)	0.5		2		3		4		5	
Condition	Avg	Range	Avg	Range	Avg	Range	Avg	Range	Avg	Range
Chlorine Req. (ppm)	1.4	0.4-2.4	3.0	1.2-4.9	3.3	1.4-5.3	3.8	1.9-5.6	5.0	3.0-6.9

Details of Disinfection System

The West Green Lake disinfection system was constructed to function as follows:

1. Three headers containing orifices, perpendicular to the shore, inject chlorinated water into the swimming area (Figs. 2, 5, and 6). When a northerly wind is blowing, producing a southerly current, the south header is closed off. When a southerly wind is blowing, the north header is closed off. Under conditions of no wind (little current) all headers are operated. The quantity of chlorinated water injected into the different areas is controlled by varying the chlorine feed rate and by use of the valves shown in Fig. 6 (pump-house plan). The amount of chlorine to be fed and the proper setting of the control valves is determined by measurements of chlorine residual in the water, the desired residuals having been determined from bacteriological tests.
2. Chlorine is distributed by the recirculation of lake water through a pump at the rate of about 500 gpm, the quantity depending upon the number of headers in use. City water would have been more desirable for this use as it has little chlorine demand, has adequate pressure to eliminate the need for a pump, does not tend to clog the orifices, and would give some desirable dilution to the lake water. However, lake water was recommended because of the possible shortage of city water if the summer was a dry one and because the cost of buying, installing, and operating a recirculation pump would be less each year than using city water (considering the commercial value of the city water). When the pump is operating efficiently, with the discharge valve or valves wide open, the discharge and gage pressure should be about as follows:

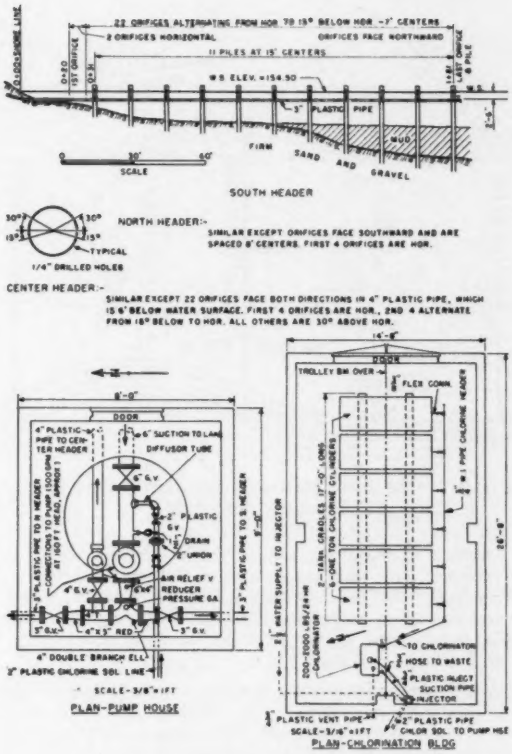

FIG. 6. DETAILS OF DISINFECTION LAYOUT

Headers Working	*Gage Press.(psi)*	*Pump Disch.(gpm)*
South or North Only	80-84	380
Central Only	65	530
South or North and Central	55-60	580
South and North	65-70	510
All Headers	40	720

3. The chlorinator is a manual machine having an operating range of 200 to 2000 lb of chlorine per 24 hr. City water at the rate of about 50 gpm is used to operate it and to inject the chlorine solution into the pump suction through 2-in. plastic pipe. Chlorine is supplied from 6 one-ton containers arranged in parallel on a central header. The use of these large containers in parallel made the purchase of an evaporator unnecessary. (A maximum of 400 lb of chlorine per day can be withdrawn from a ton cylinder without the use of an evaporator, which costs about $2300.) An empty cylinder alarm was used instead of the costly scales. Arrangements were made with the City Water Department to deliver the chlorine cylinders since they are

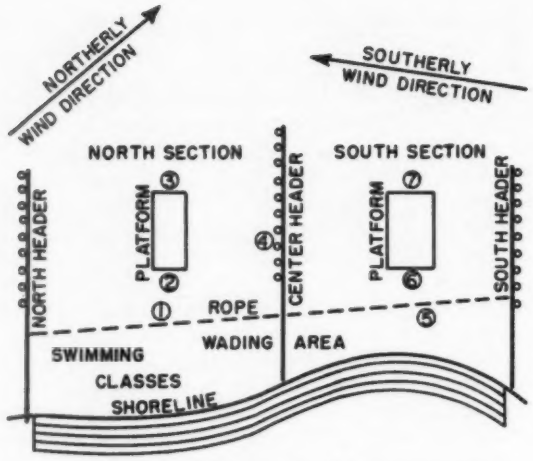

FIG. 7. CHLORINE RESIDUAL AND BACTERIOLOGICAL SAMPLING STATIONS

identical to those obtained by the Water Department on contract. The chlorinator was started each morning in sufficient time for the build-up of 0.3 ppm of chlorine residual before swimming commenced. A separate building was erected for the chlorinator and chlorine cylinders as indicated in Figs. 5 and 6.

4. A 500-gpm recirculation pump (an iron-body turbine type with 160-ft head) powered by a 220/440-v electric motor was installed in a pump and control house located in front of the bathhouse (Fig. 5). The pumphouse floor was depressed 5 ft below the ground surface to reduce the building's visible height and the length of pump shaft required. Electric conduits to the pumphouse were buried. Three plastic valves to control the chlorine dosage to each distribution line are located in the pumphouse. A 6-in. pump suction line extends into 10 ft of water between the diving platforms.
5. The chlorine diffuser lines or headers are plastic pipes supported from piling driven on 15-ft centers. This type of support permits easy removal of the pipe for cleaning, adjustment, or repairs. The headers on the north and south boundary of the bathing area are located 30 in. below the water surface; the center header is 6 ft below the water surface where it is opposite the diving platforms. Orifice details for the headers are shown in Fig. 6. To permit flushing for cleaning, each header has a valve at its outboard end. All pipe on land and near the water's edge is buried. Signs are posted on the piling asking swimmers to stay off the pipe and to keep away from the piling.
6. The complete equipment and construction cost for the facility was $33,949.

Operating Requirements

The chlorination facility was placed in operation on June 16, 1959, with control of the operation under the head lifeguard and the Evan's Pool maintenance personnel. The arrangement did not prove satisfactory; so a full-time operator (a University student) was hired on June 24 for the remainder of the swimming season. This operator had these duties: (1) starting the pump and chlorinator about ½ hr before the beach opened so that a chlorine residual of approximately 0.3 ppm could be built up prior to the commencement of bathing and swimming; (2) collecting chlorine-residual samples every ½ to 2 hr, depending upon the conditions, at 6-in. and 6-ft depths from the 7 stations shown in Fig. 7; (3) adjusting the chlorinator feed rate and header-control valves to give the desired chlorine residual in the beach areas where there were swimmers and bathers; (4) collecting periodic samples for bacteriological analysis; (5) keeping a running record of the operation as shown in Table I; (6) maintaining the system by flushing the headers, pumping out the pump pit, and changing chlorine cylinders; and (7) shutting the system down at the close of the swimming day.

The total cost of about $1930 for the 1959 season included operation, $1100; chlorine, $650; and power, $178.

Operating Conditions

The amount of chlorine required for disinfection varies with the sections of the beach area being used, the wind direction and velocity, the amount of sunlight, the water quality, and the number of bathers in the water. The lifeguards limit the bathers and swimmers to designated areas, depending upon the number present. With 20 or fewer bathers, they are limited to the south end of the south section; with 20 to 100, they are limited to the south section; and with over 100, the entire beach area is opened. Swimming classes are held inside the rope along the north section. Only the south header need be operated when the wind is southerly and just the south section is in use. If there is no wind, the central or the central and south headers should be operated. A northerly wind usually means a good day for swimming, and the entire beach area is open; then all three headers or the north and central headers are used.

Table I is a sample from the record sheets that summarize the chlorination plant operation and the chlorine residuals obtained in 1959. This sampling from the summary sheets for 72 days shows the record for 14 days during the peak of the bathing season. On the average, about 60 separate chlorine-residual readings were taken each day. After discovery that the central header had been installed upside down, it was realigned on July 1. The north header outboard of the fifth piling (last half) is turned so that the orifices all point downward instead of alternating between horizontal and 15° below horizontal. This misalignment should be corrected before the next swimming season. With the realignment a gate valve should be installed about midway in this header

TABLE I

SAMPLE FROM WEST GREEN LAKE
CHLORINATION SUMMARY (JULY 26-AUG. 8, 1959)

Date	Wind	No. of Bathers*	Cl_2 Feed Range (Lb.)	Cl_2 Used (Lb.)	Operation (hr.)	mg/l Avg. Chlorine Residual at Sampling Sta.†							Headers in Operation
						1	2	3	4	5	6	7	
7-26-59	NW	20-300	4-500	2057	9	0.45	0.35	0.2	0.6	0.7	0.5	0.4	C
27	Rain-S	0-20	2-600	2202	9	0.2	0.15	0.1	0.2	0.35	0.2	0.1	S
28	NW	20-250	5-900	2457	9	0.1	0.1	0.1	0.5	0.7	0.4	0.3	C
29	NW	10-200	5-600	2663	9	0.2	0.15	0.1	0.5	0.75	0.6	0.2	C
30	NW-N	50-400	5-900	2949	8.5	0.2	0.1	0.1	0.75	0.6	0.4	0.2	N & C
31	W-NW	60-500	7-1000	3259	9	0.3	0.2	0.2	1.0	0.4	0.25	0.15	NC & CS
8-1-59	S	0-150	2-700	3443	9	0.15	0.1	0.1	0.1	0.75	0.4	0.2	CS & S
2	S-SW	0-50	2-700	3651	8.5	0.2	0.15	1.15	0.5	0.75	0.25	0.15	CS & S
3	SW	0-150	3-800	3911	9	0.2	0.1	0.1	0.15	0.7	0.3	0.2	S
4	NW	0-10	2-700	4061	9	0.05	0.05	0.05	0.2	0.5	0.2	0.15	C
5	W	20-200	6-700	4311	9	0.5	0.35	0.3	0.75	0.8	0.5	0.3	C
6	NW-N	20-300	6.5-1100	4607	9	0.2	0.25	0.2	0.7	0.75	0.5	0.3	NC & C
7	NW-N	30-200	6.5-1100	4898	9	0.8	0.4	0.4	0.7	0.75	0.5	0.2	NCS & C
8	NW-N	5-400	7-800	5167	9	0.4	0.3	0.3	0.6	0.75	0.6	0.3	C

* Number of bathers shown is the actual count of those in the water (range) at any one time during the day.
† The number of chlorine residuals taken daily from each sampling station varied between 6 and 16. Stations 2, 3, 6, and 7 were sampled from near the surface and at mid-depth. Chlorine residual was allowed to decline at stations 1, 2, and 3 when the lifeguards restricted swimming to the south portion of the beach. This was the case during periods of low swimming population.

so that chlorine can be shut off in its outer half when there is no swimming beyond the ropes in this section of the beach.

A total of about 15,200 lb of chlorine was used in 1959 for 72 days of swimming, or an average of 211 lb per day. The rate of chlorine feed ranged from 200 to 1100 lb per 24 hr; an average operating day was about 8.5 hr.

On one occasion the intake screen was lifted off the end of the suction pipe by a group of boys; and shortly thereafter the pump lost its suction, chlorine continued to feed into the system, and the odor of chlorine became pronounced in parts of the swimming area. After shutting down the system, police skin divers replaced the screen, and the facility was returned to operation. The recirculation pump later developed a serious vibration, and it was shut down on September 2. After its removal, the pump impeller was found to be seriously corroded by the chlorine fed into the pump suction when the pump was not pumping water. An automatic switch and alarm to be installed will shut off the pump and the chlorinator if ever again the pump loses its suction.

Operating Results

The chlorination facility operated very well with the exception of the troubles mentioned in the preceding section. There were no complaints of eye smarting or chlorine odors. A few dozen trout were killed on the first day of operation, but no kills of any significance were reported thereafter. The West Green Lake Beach was one of the most popular in King County. As shown in Table II, it had the best bacteriological record of the six beaches in King County sampled during the summer of 1959 by the King County Health Department. Coliform bacteria

TABLE II

BATHING-BEACH BACTERIOLOGICAL DATA*
KING COUNTY, JUNE 25 - SEPT. 2, 1959

	GREEN LAKE		LAKE WASHINGTON		PUGET SOUND GOLDEN GARDENS	LAKE SAMMAMISH STATE PARK
	WEST BEACH	EAST BEACH	SEWARD PARK	JUANITA		
No. of values	113	105	113	113	112	113
Median value†	23	230	230	60	230	60
Range of values	0 to 2400	0 to 24,000	0 to 13,000	0 to 7000	0 to 7000	0 to 2400
Avg No. bathers	130	104	110	110	43	114
Avg water temp.	70.3	71.1	69.0	70.5	58.2	71.9
Coliform per bather‡	0.18	2.2	2.1	0.54	5.4	0.53

* Most probable number of coliform bacteria per 100-ml sample, computed from Seattle-King Co. Health Dept. data.
† Less than 45 proportioned equally among 0, 15, 30, and 45.
‡ Coliform per bathers $= \frac{\text{Median}}{\text{Avg No. Bathers}}$.

TABLE III

STATISTICAL ANALYSIS OF GREEN LAKE BACTERIOLOGICAL DATA, JUNE 25-SEPT. 2, 1959

SOURCE	ARITHMETIC MEAN	GEOMETRIC MEAN	MEDIAN	STANDARD DEVIATION	COEF OF VARIATION OF GEO. MEAN	RANGE CONTAINING 50% OF VALUES
West Beach*	105¶	30	23	4.48	0.15	11-83
West Beach†	20.7	2.21	2	11.35	5.14	0-13.6
West Beach‡	7.06	3.94	4	4.11	1.04	1.48-10.2
East Beach*	1011¶	196	230	6.74	0.32	55-720
East Beach†	27.9	16.2	14	3.72	0.23	11.25-23.4
East Beach‡	9.81	4.06	3.6	12.0	2.96	0-21.8
Green Lake§	17.5	3.16	3.6	14.41	4.56	0-19.1

* Seattle-King Co. H. D. data: 113 samples at W. Beach, 105 samples at E. Beach.
† U. of Washington data: 67 samples at W. Beach, 38 samples at E. Beach.
‡ U. of Washington data: 30-39 samples obtained just outside bathing area and up wind.
§ U. of Washington data: 94 samples obtained at regular sampling stations—all outside bathing areas.
¶ Values influenced by a few extreme coliform densities.

concentrations were very low, the median being less than one-tenth of the tolerable limit of 240[4] established by the State Health Department for Washington water. A normal tolerable limit of 1000 is used in California and many other states.[5*] If the average chlorine residual can be kept between 0.4 and 0.6 ppm during the next swimming season, the coliform bacterial density in the bathing and swimming areas should be even better. It should be noted that the coliform bacteria are merely indicators of water quality.

The following comparison, which applies to Table II, points up the record for the six King County beaches mentioned in the preceding paragraph:

1. The West Green Lake Beach had the highest water quality (bacteriological) and the most bathers.
2. The East Green Lake Beach (unchlorinated) had coliform concentrations greater than Juanita Beach on Lake Washington and greater than the Lake Sammamish State Park. It was comparable with Seward Park on Lake Washington and Golden Gardens on Puget Sound.
3. Golden Gardens bacteriological data are influenced by the nearby North Trunk Sewer Outfall and the discharge from the Ship Canal.
4. The water temperature at all beaches was about the same except for Golden Gardens, where it was 12° cooler.

Table III presents a statistical analysis of coliform bacteria densities observed at the two Green Lake bathing beaches by the University and by the Seattle-King County Health Department during the 1959 bathing season. Health Department samples were collected in the area of greatest swimming concentration, three samples being taken (surface, middle, and bottom) at knee depth and a similar three at a depth of 5 ft. University samples were collected from 6-in. and 6-ft depths in three locations—outside and upwind of the swimming area (control samples), in the wading area, and around the platform where most swimmers were congregated. Table III also shows the bacteria densities obtained from throughout the Lake (exclusive of bathing areas) for the same time period. The data in Table III are the basis for a comparison of the chlorinated water at West Beach and the untreated water at East Beach:

1. The bacteria concentration was sufficiently low for swimming at both beaches.
2. The bacterial densities at the West Beach were one-seventh to one-tenth of those at the East Beach.
3. The water quality inside the swimming area at the West Beach was about the same as that outside the swimming area, despite the presence of many bathers.
4. The coliform concentration at the East Beach was about three to four times as high inside the swimming area as outside it, though the count for the inside area is not high. The bathers contributed these additional bacteria.
5. The water quality in the swimming areas did not differ markedly (according to University data) from that of the lake water in general, indicating the large water exchange brought about by wind-induced currents.
6. University data gave lower values than did the Health Department data because of a difference in the sampling points.
7. The statistical evaluation was hampered by a large number of zero values and by many Health Department values that were recorded as "less than 45."

Recommendations Made to the City

Now that the North Trunk Sewer has been repaired, it is unlikely that any more sewage will be discharged into Green Lake. The Lake has also purified itself of former sewage discharges. However, a great many persons have become skeptical of the water quality of the local beaches and are fearful about swimming in any natural body of water. Others will, of course, swim anywhere at any time. By providing one natural bathing area with a controlled bacteriological quality, the City would be making a truly worthwhile contribution to the general well-being of these many people who wish to swim in a natural setting but are hesitant to do so because of

(Continued on page 32)

* These limiting values usually apply to bacteria from humans rather than from wild life. But the bacteria found in Green Lake during the 1959 season were largely from wild life; and they have a different sanitary significance from those that come from humans.

On the Brittle Fracture of Structures

PAUL C. PARIS
Assistant Professor of Civil Engineering

WILLIAM E. ANDERSON
Research Engineer, The Boeing Airplane Company

P. C. Paris

Galileo in 1638 gave a lucid description of the character of internal forces that resist separation within material bodies.[1] Since his time only two significant types of separation or fracture theories have been proposed. The first is the concept that the "state of stress" at a point may be regarded as the cause of incipient fracturing. Coulomb in 1776 made use of this idea to describe material failures. This concept has been carried down to date as a criterion of yielding at a point in a body; however, it has not been successful in describing the "brittle failures" of many structures over the past century.

The second theory proposes that all materials and structures contain flaws and that under load the worst of these flaws will grow, causing fracture. Griffith in 1920 developed the first successful theory of flaw growth in brittle solids.[2] His methods have been modified and developed as a criterion of "brittle fracture" of ductile materials, especially by Irwin.[3] These relatively new concepts are presently employed by the aircraft industry and others in analyzing fractures in structures composed of ductile metals. The choice of materials for aircraft structures is based in part on the results of these modern fracture analyses. Hence this article will attempt to describe these theories and to illustrate a few applications, as well as to indicate some of the current trends in fracture analysis.

Griffith Theory Applied to Ductile Materials

Griffith derived a stability criterion for flaws (cracks) in ideally brittle materials such as glass. He reasoned that a crack in a plate of material will grow if the energy supplied from the stress field, $\mathcal{G}$, exceeds the surface energy of the new crack surface, $2T$,* during an increment of extension. Hence for the commencement of instability,

$$\mathcal{G}=2T. \qquad (1)$$

Using stress analysis to compute $\mathcal{G}$ for the configuration shown in Fig. 1, he found that

$$\frac{\pi\sigma^2 a}{E}=2T \qquad (2)$$

or

$$\sigma\sqrt{a}=\sqrt{\frac{2TE}{\pi}} \qquad (3)$$

W. E. Anderson

Now, the right side of Eq. (3) is a material constant; hence flaw stability depends on both stress level and flaw size.

The tip of a crack has a theoretical stress-concentration factor approaching infinity; hence in ductile materials a zone of yielded material always accompanies a crack tip. As the crack extends, plastic deformation occurs that dissipates energy. This adds to the surface energy, $2T$.

Equations (1) through (3) can be modified by the additional term, dP/dA, the plastic work per unit of crack surface area created in crack extension. From

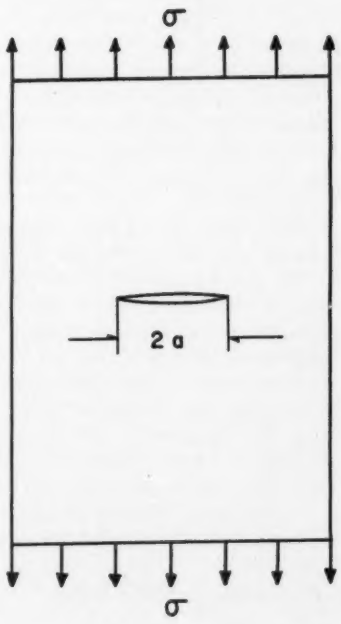

FIG. 1. THE GRIFFITH CONFIGURATION

* A 2 is required with T since the surface area of both faces of a crack must be considered.

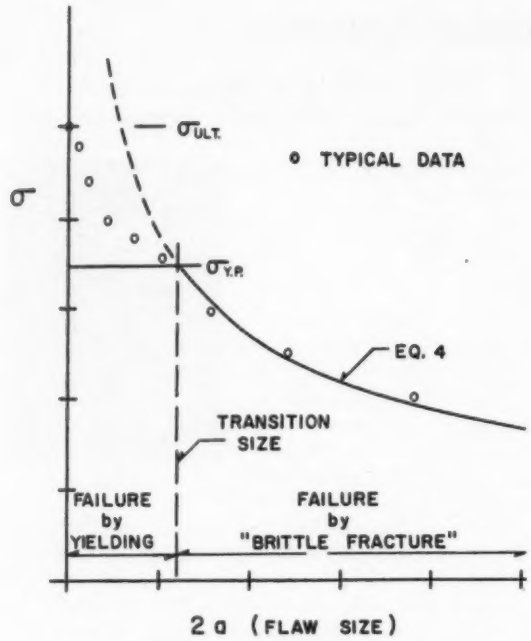

FIG. 2. TYPICAL CRACKED-STRENGTH BEHAVIOR

these considerations, Eq. (3) becomes

$$\sigma \sqrt{a} = \sqrt{\frac{(2T + \frac{dP}{dA})\, E}{\pi}} \quad . \qquad (4)$$

Experiments and additional theoretical considerations show that dP/dA is a constant for a given thickness of a material provided that the nominal stress level, σ, is below the yield point, σ_{yp}. Moreover, $2T$ is negligibly small compared to dP/dA in ductile metals.

Figure 2 shows Eq. (4) plotted for a typical material. By using severe yielding as a criterion of failure also, the curve is cut off at the yield point of the material. If a structure contains flaws larger than the transition size, brittle fracture occurs rather than gross yielding when the structure is overloaded. Such behavior is undesirable in that the structure should be able to dissipate the energy of occasional overloads without the occurrence of fracturing. Moreover, the Theory of Plastic Design indicates that the ability of structural components to yield rather than to fracture allows a redistribution of forces in redundant structures that enhances their strength.

So-Called High-Strength Metal Alloys

The common alloys of aluminum used in aircraft structures are numbered 2024-T3, 7075-T6, and

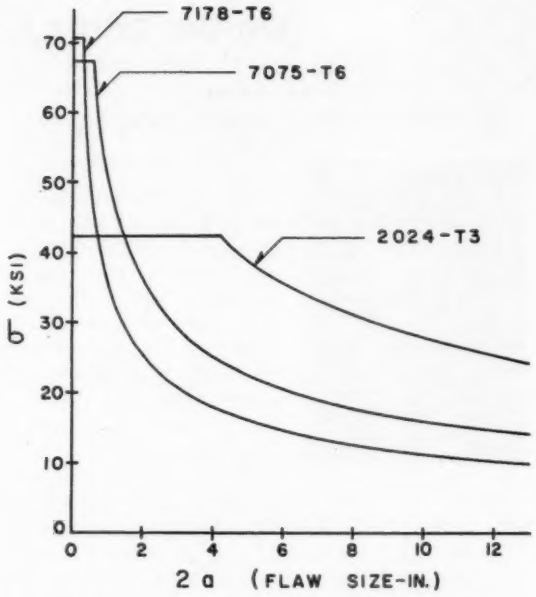

FIG. 3. COMPARISON OF COMMON ALUMINUM ALLOYS

7178-T6. The latter two are often called "high-strength" alloys because their tensile yield strengths are half again higher than 2024-T3. However, their dP/dA values are considerably less than 2024-T3. Curves of their behaviors that have been prepared (in the manner of Fig. 2) are superimposed in Fig. 3. (A sheet thickness of 0.064 was selected as a typical gage for Fig. 3, and the required data were furnished by the Boeing Airplane Company.)

As can be seen in Fig. 3, the so-called high-strength alloys are stronger only if flaws are very small. Since accidental damage or fatigue cracks are likely to occur during the service life, 2024-T3 is a much safer alloy for airframes.

Thus modern trends toward higher-strength metal alloys in all types of structures will require special considerations of the possibility of brittle fracture. Special tests must be performed to evaluate the tear resistance (i.e., dP/dA) of materials for such judgments, since tensile stress-strain tests supply only the "no flaw" properties.

The Role of the Structural Engineer

Traditionally, the metallurgist is consulted when brittle failure occurs. However, since structural details have a great influence on brittle behavior, the design responsibility of the structural engineer cannot be neglected. For example, consider the behavior of a small crack emanating from the corner of a cutout.

If the cutout is unreinforced, as shown in Fig. 4, the crack length, $2a$, which should be used in Eq. (4)

for analysis, should include the width of the cutout. Hence very small cracks can cause brittle fracture. However, if the cutout is properly reinforced, the effective crack length can be considerably reduced.

The tendency toward brittle fracture in a structure can be affected more by the design of structural details than any other factor. Recent ship failures, wherein cracks have emanated from hatch openings, and the failures of the deHaviland "Comet" fuselages by cracking from a window cutout are evidence that the structural engineer is only now becoming aware of these problems. The role the structural engineer must play is clear:

1. He must obtain data from the metallurgist on the fracture properties (i.e., dP/dA) before making the choice of materials for a proposed structure.
2. He must anticipate the possibility of flaws and cracks, such as fatigue cracks or damage from other sources, and provide structural details so that undetected flaws will not cause catastrophic failures.
3. He must provide the persons servicing his structure with information on the flaw size or amount of damage the structure may safely sustain, in order that proper inspections may be executed.

At present, aircraft structural design is performed by using this threefold procedure. The most difficult step is that of anticipating and analyzing cracks. Current research is providing stress analyses of many structural configurations containing cracks, such as was necessary to compute the left-hand side of Eq. (2). These analyses require the application of Theory of Elasticity and other advanced principles.

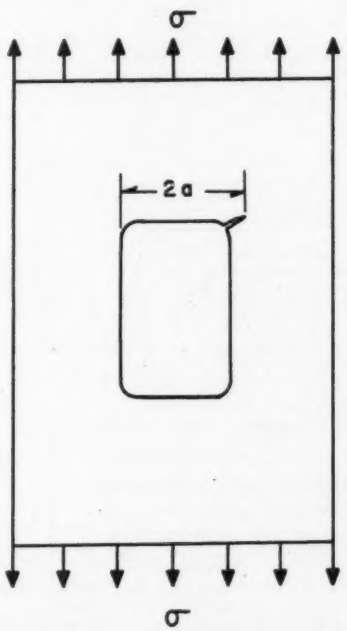

FIG. 4. EFFECTIVE CRACK SIZE IN UNREINFORCED CUTOUT

The results of these studies are tabulated throughout the literature for the convenience of the design engineer, and many approximate methods of analysis are now available. It remains to find simple code-type specifications to avoid brittle fracture.

In the future, the structural engineer will do more than simply obtain data from the metallurgist on material properties. Through a mutual understanding of the problems of design to avoid brittle fracturing, a more judicious choice of structural materials may be accomplished. This is to say that the structure itself may incorporate materials designed for specific applications. Hence a discussion of the materials-behavior aspects of the problem of brittle fracture is pertinent.

Factors Affecting Tear Resistance

The energy-dissipating capacity of a cracked material is the factor measured by the term dP/dA. This capacity is effectively due to plastic flow at and around the crack tip; so a study of this plasticity is desirable. Consideration begins on a microscopic level.

In almost all materials a shear stress of some magnitude must occur so as to cause plastic flow. The operating deformation system in any given material usually consists of multidimensional and increasingly complex modes. Systems tend to resist further deformation all the while they are being deformed by the shear forces.

Commonly used solid materials try to maintain contiguity with themselves; i.e., they resist the development of free surfaces. The deformation systems thus tend to operate in a way that will maintain compatability with adjacent systems. Clearly, the activity of a system is influenced by the activity of its neighbors.

These activities at the microscopic level are influenced by the larger stress state imposed on them. Consider the region around the crack tip in a material of thickness involving a few tens of systems, all of which is in a state of plane stress. Early plasticity is accomplished by initial or easy-shear modes. With further stretching the material thins by realigning of the systems. Increasingly complex modes can be made to operate by the shear loads imposed on one system by its neighbor. The multidimensionality of the energy-dissipating systems provides a large amount of deformation. Associated with this is a large value of tear resistance.

If the thickness of the material is reduced markedly, the number of systems is also markedly reduced. Under a similar state of plane stress, the interference of one deforming system with its neighbor is reduced. Fewer of the more complex deformation modes are achieved by the several systems. The

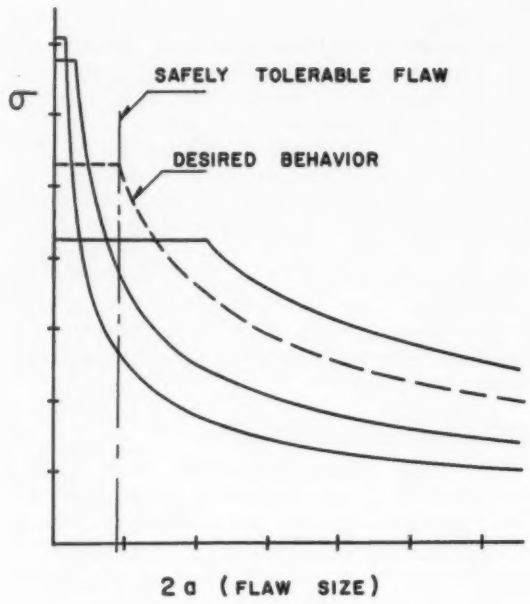

FIG. 5. OPTIMUM BEHAVIOR FOR GIVEN FLAW SIZE

relative capacity to absorb energy is reduced and the thinner material will have less tear resistance than before.

If the thickness is vastly increased, a state of plane strain occurs in the material around the end of the crack. This means that the material is not subjected to much shear. Fewer deformation systems will operate; and tear resistance will be lowered.

The previous discussion is intended to be generally applicable to any plastically deformable solid. Knowledge of the mechanisms of deformation will allow an estimate of the plastic work dissipation by the given material in the given condition. The fracture mechanics of an acrylic window or a clay bank may not be less important than fracture of a structural pressure vessel, but the final discussion will be restricted to commercial metal alloys used in structural applications.

Alloy Design for Optimum Tear Resistance

The selection of a metal for a structural function is normally based on cost, weight, mechanical properties, and availability of suitable shapes. Alloy or processing changes can be made that will affect mechanical properties without significant changes in the other factors. This will be called alloy design.

Important mechanical properities are yield strength and elastic stiffness. Gross changes in elastic stiffness cannot be effected, but the opposite is true for yielding. The yield strengths in some important cases can be altered by an order of magnitude. Since yielding behavior will affect tear resistances as well as other design considerations, a more detailed examination of this situation is desirable.

Reconsider the curves shown as solid lines in Fig. 3. If the anticipated flaw size that can be safely tolerated in a certain component is as shown in Fig. 5, 7075-T6 is not safe, but 2024-T3 is too safe. Therefore it would be desirable to design an alloy that would have the property shown by the heavy dotted line.

It is possible to modify the thermal and mechanical processing of 2024 to achieve behavioral changes in the desired direction, although slight alteration of the composition may be necessary to obtain optimum combinations of yield strength and tear resistance. The metallurgical factors involved are based on selective precipitation. Such changes are possible in any of the metallic systems that employ controlled precipitation for strength gains. Fortunately, considerable basic information is now available about the precipitation mechanisms. But the determination of absolute changes in yielding and tear resistance depend on carefully planned experiments. The near future will see some results from present efforts in this direction, as commercial advantages from successful use of these concepts can be most rewarding.

REFERENCES

1. GALILEO GALILEI, *Two New Sciences*, 1638 (Translation published by Dover Pub. Inc., New York City).
2. A. A. GRIFFITH, "The Phenomena of Flow and Rupture of Solids," *Phil. Trans. Roy. Soc. of London*, Vol. 221, 1921.
3. G. R. IRWIN, "Fracture," *Handbuch der Physik*, Vol. VI, Springer, 1958.

Information Wholesale: At VINITI—the Soviet centralized information services—the editors estimate that over 700,000 abstracts of scientific articles will have been published in 1959; these will have appeared in 13 abstract periodicals, which draw from 12,000 journals and 3000 special Soviet publications issued in 95 countries and 65 languages. *Chemical and Engineering News*, Jan. 11, 1960, p. 70.

Lunar Tidal Variations in the Ionospheric Layers*

N. NARAYANA RAO
Graduate Student in Electrical Engineering

H. MYRON SWARM
Professor of Electrical Engineering

N. N. Rao

It has been known for many years that the ionospheric layers are subject to tidal variations. In order to explain how lunar tidal variations affect the ionosphere, we need to know the meaning of the word *tide* and to understand the behavior of the ionosphere. Although tides are commonly associated with the oscillatory motion produced in the ocean by the gravitational pulls of the moon and the sun, the same term is applicable to the atmospheric movements. However, there is a fundamental difference between ocean and atmospheric tides. The movements of the water are mainly horizontal, whereas in the atmosphere the movements are more complicated, due to the compressibility of the gases. The tidal motions can have different velocities, both horizontal and vertical, and even different directions at different heights. The effect of the earth's magnetic field further complicates the tidal phenomenon in the ionosphere.

The term *ionosphere* applies to the region of the upper atmosphere extending from a height of about 60 km up to about 500 km above the earth. As the name implies, the region consists of ionized gases, primarily caused by the solar ultraviolet radiation. The density of ionization is not uniform with height, and there are distinct layers with corresponding maximum ionizations. These are named D, E, F_1, and F_2 layers. Figure 1 shows the approximate locations of these layers and the corresponding electron densities. Besides these normally regular layers, a sporadic E layer (known as E_s) frequently exists. These ionized layers often behave like reflectors of radio-frequency energy, by bending the waves and returning them to earth through a process of refraction. However, if the frequency of the wave is increased beyond a certain limit, depending upon the value of maximum electron density of a layer and the angle of incidence of the wave upon the layer, the wave may penetrate through the layer. The highest vertically incident wave frequency that can be reflected from the height of maximum ionization density of any layer is defined as the "critical frequency" of that layer. The critical frequency is hence dependent upon the value of maximum ionization density of the layer.

H. M. Swarm

The purpose of this paper is to evaluate theoretically the effects of lunar tides upon the ionospheric parameters and to compare the theoretical with the experimental results.

IONOSPHERIC DATA

The following nomenclature is appropriate for the ionospheric parameters, some of which are obtainable by using a sweep-frequency ionospheric recorder of the type described in the July, 1958, issue of *Trend* by Swarm *et al*[1]:

$h'E(E_s, F_1 \text{ and } F_2)$ = the minimum equivalent height of reflection of the $E(E_s, F_1, \text{ and } F_2)$ layer,

$h_{max}E(F_1 \text{ and } F_2)$ = the height of maximum ionization of the $E(F_1 \text{ and } F_2)$ layer, and

$f_oE(F_1 \text{ and } F_2)$ = the critical frequency of the $E(F_1 \text{ and } F_2)$ layer.

In brief, the method of collecting data is to send a pulse of radio-frequency energy vertically upwards and measure the time delay between the transmitted pulse and the pulse received after reflection from the ionosphere. If this time delay is multiplied by the velocity of light, the result gives the "equivalent" or "virtual" height at which the pulse is reflected back to the earth. This is not equal to the "actual" or true height, since the velocity of propagation of the pulse through the ionized region is reduced, especially as the incident wave frequency approaches the critical frequency of the layer. By varying the frequency of

* This article is based on Mr. Rao's thesis submitted as partial fulfillment of the requirements for the degree of M.S. in Electrical Engineering. The authors wish to express their thanks to the Engineering Experiment Station of the University of Washington for the financial assistance rendered during the course of the investigation upon which the article is based.

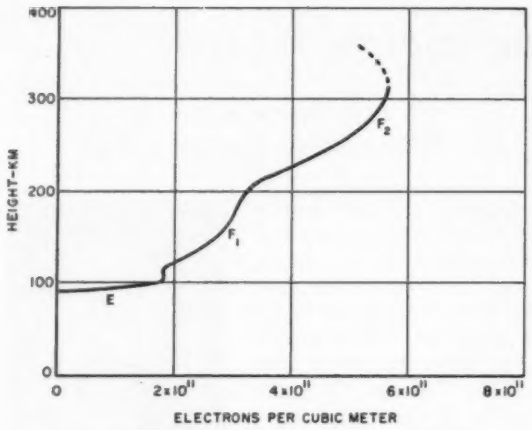

FIG. 1. A TYPICAL MODEL OF THE IONOSPHERE

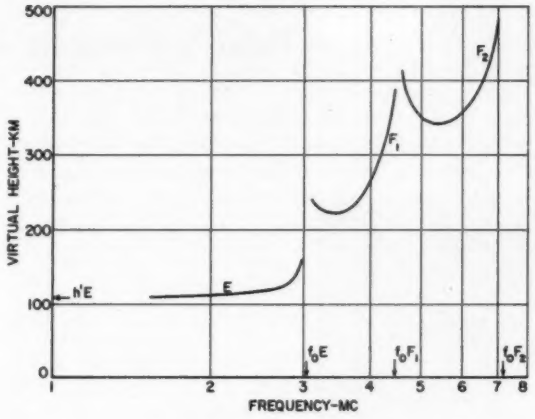

FIG. 2. A TYPICAL IONOGRAM

the transmitted pulse, a virtual height-vs-frequency record—an *ionogram*—may be obtained. Figure 2 is a representation of such an ionogram, redrawn for clarity. As is apparent from the figure, the minimum equivalent heights of reflection and the critical frequencies can be directly ascertained from the ionogram. The approximate true heights of maximum ionization, h_{max}, are equal to the virtual heights read off the ionogram at a frequency 0.834 times f_o, according to Booker and Seaton[2].

THE TIDAL PHENOMENON

The distribution of ionization of the ionospheric layers undergoes regular diurnal, seasonal, and sunspot cycle variations, and these are quite different at different geographical locations. All these effects are largely a result of changes in the ionizing radiation; but to a lesser extent they are also due to tides. In fact, some of the peculiarities of the F_2 layer are explainable by the tidal phenomenon, and this is one of the main reasons for intensive research in this field. The tidal effects are concealed in the variations of h', h_{max}, and f_o of the ionospheric layers, which are the sum of contributions owing to the sun and moon. Fortunately, the lunar tidal variations—unlike the solar ones—are easily separable. The reason is that the periods of lunar variations average 24 hr, 51 min and its simple submultiples, whereas the periods of solar variations coincide exactly with those already present in the ionospheric data, from the simplest considerations of electron production. The semidiurnal lunar variation of period 12 hr, 25.5 min has been observed to possess the strongest amplitude.

The lunar tidal phenomenon in the ionosphere may be obtained quantitatively by calculating the amplitudes and phases of semidiurnal sinusoidal variations (of period 12 hr, 25.5 min) in the ionospheric parameters h', h_{max}, and f_o, after the solar effects have been removed. This process has been described by Swarm *et al*[1]. Several research workers have applied this method to the experimental ionospheric data at different geographical locations. The results of these studies, which mostly deal with $h'E$, $h'E_s$, $h_{max}F_2$, and f_oF_2 variations, are shown in Tables I and II. The nomenclature is as follows:

P_2 = amplitude of the semidiurnal lunar variation in the height,

t_2 = phase of the semidiurnal lunar variations (after lunar transit), and

$\frac{200\,P_2}{f_oF_2}$ = amplitude of the semidiurnal lunar variations in the maximum electron density of the F_2 layer.

For convenience, the critical frequency variations have been presented as percentage variation in the maximum electron density.

So far, the presentation has dealt with the evidence of lunar tides in the ionosphere from an experimental researcher's point of view. If we now consider the lunar semidiurnal tidal theory and its consequences on the ionospheric parameters, we can compare the results of the theoretical treatment with the experimental results, and can evaluate any discrepancies between the two.

IONOSPHERIC TIDAL THEORY

The foundation for the ionospheric tidal theory was laid in 1882, even before the experimental discovery of the ionosphere, when Balfour Stewart[3] suggested that certain terrestrial magnetic variations were an indirect manifestation of the tidal motions in the upper atmosphere. Stewart's theory has become widely known as the "dynamo theory" of magnetic

TABLE I

HARMONIC COEFFICIENTS OF SEMIDIURNAL LUNAR VARIATIONS IN F_2-REGION DATA

LOCATION	GEOMAGNETIC LATITUDE	RESEARCHER	h_mF_2			f_oF_2		
			P_2(km)	t_2(hr.)	MONTHS OF DATA	$\frac{200\,P_2}{f_oF_2}$	t_2(hr)	MONTHS OF DATA
Huancayo	1° S	Martyn	5.2	8.4	30	3.4	4.3	36
Ibadan	10° N	Brown	7.7	8.1	40	...	4.3	40
Calcutta	12° N	Baral	2.0	4.0	36	...	...	...
Kihei	21° N	Martyn	...	...	...	...	0.1	14
Cape York	21° S	Martyn	3.5	6.4	6	2.7	9.4	36
Durbanville	33° S	Martyn	...	...	...	2.6	11.8	8
Brisbane	36° S	Martyn	3.6	5.5	27	2.8	9.3	30
Washington	41° S	Martyn	2.0	6.9	84	2.2	10.4	112
Canberra	44° S	Martyn	1.7	5.7	36	2.7	9.4	36
Christchurch	48° S	Martyn	...	...	...	2.6	8.5	28
Washington	50° N	Martyn	...	...	...	...	11.0	12
Hobart	52° S	Martyn	2.2	7.5	9	2.4	9.3	10
Slough	55° N	Appleton and Benyon	2.0	6.0	...	...	11.0	12
Ottawa	56° N	Martyn	...	...	...	...	11.4	30

TABLE II

HARMONIC COEFFICIENTS OF SEMIDIURNAL LUNAR VARIATIONS IN E-REGION DATA FOR VARIOUS SITES

LOCATION	GEOMAGNETIC LATITUDE	INVESTIGATOR	LAYER	NUMBER OF MONTHS	P_2(km)	t_2(hr)
Huancayo	1° S	Matsushita	E_s	13	0.19	1.3
Ibadan	10° N	Wright and Skinner	E_s	12	0.22	7.0
Brisbane	36° S	Martyn	E and E_s	..	0.50	4.5
Brisbane	36° S	Matsushita	E_s	13	0.70	5.7
Brisbane	36° S	Thomas and Swenson	E_s	10	0.69	6.7
Brisbane	36° S	Gazzard	E_{2s}	22	1.50	1.5
Canberra	44° S	Martyn	E	..	0.19	5.1
Stanford	44° N	Swarm and Helliwell	E_s	6	0.59	6.4
Washington	50° N	Matsushita	E_s	13	0.46	5.8
Slough	55° N	Appleton and Weekes	E	11	0.93	11.2
Ottawa	56° N	Datars	E	..	0.40	9.5
Ottawa	56° N	Jelly	E	12	0.50	0.5-5.9

variations. According to this, the daily solar and lunar magnetic variations are caused by horizontal tidal movements of the conducting upper atmosphere across the magnetic field of the earth. The conducting ionized region of the upper atmosphere may be pictured as the armature of the atmospheric dynamo, the earth being its permanent field magnet and the atmosphere carrying the conducting layer, the rotor. If a conductor moves with a velocity v in a direction at right angles to a magnetic field of intensity B, then an emf E is induced in the conductor, given by $E = Bv$ per unit length of the conductor, where E, v, and B are components along the positive directions of x, y, and z axes of a right-handed coordinate system. The induced electromotive forces, perpendicular to the earth's magnetic field, then direct the positively charged particles in the opposite direction to the negative particles and set up a system of electric currents, which in turn are responsible for the terrestrial magnetic variations.

Early recognition was given to the dynamo theory by Schuster[4] and Chapman[5] in their work on the terrestrial solar and lunar diurnal magnetic variations. However, when the ionosphere was discovered experimentally, about 1925, by Appleton and by Breit and Tuve, the theory was confronted with serious quantitative discrepancies, in the conductivity of the ionosphere and in the velocity of the horizontal tidal winds. These difficulties were, to some extent, more apparent than real, since in calculating the electromotive forces caused by tidal motions the wind velocities have been deduced from the observed amplitudes of the barometric oscillations near the ground. In 1936, when Taylor[6] and Pekeris[7] showed that in the general case of temperature gradient the wind velocities in the upper atmosphere could be much larger than those at the ground, the difficulties were only partly removed.

In 1932 Cowling[8] pointed out that intense polarization fields can be established by the currents, in suitable circumstances. These fields can play a more important part than the original induced electromotive forces in determining the ultimate pattern and strength of the current flow. Then it became apparent that the polarization fields can lead to a substantial increase in the effective conductivity, which relates the ultimate currents to the primary emf. On this basis, Stewart's dynamo theory was subject to modifications by Baker and Martyn[9,10,11], and independently by Hirono[12] and Fejer[13]. The remainder of this paper extends the work of Baker and Martyn[9,10,11]. Their modification of the classical dynamo theory will henceforth be referred to as the "revised dynamo theory."

The revised dynamo problem assumes the density of ionization in the upper atmosphere to be independent of geographical position, the density being a function of height only, and thus treats the ionosphere as a series of spherical shells surrounding the earth. The anisotropic conductivity of the ionosphere with regard to height is included in the theory. The geographical latitude variation is simplified by dividing the region between the geomagnetic equator and the geomagnetic poles into two zones of isotropic conductivity. One of these zones is an equatorial strip 3° wide on either side of the geomagnetic equator that has been found to be effectively a better conductor than the other zone. The increased conductivity of the equatorial zone is effective in the east-west direction, as has been confirmed[14] experimentally. The height variation of the conductivity, as calculated by Baker and Martyn, indicates the ionosphere to be a better conductor at E-region heights than at other heights. The height of maximum conductivity was found to lie between 100 km to 110 km above the earth's surface. Results of experimental observations with rocket-borne magnetometers obtained by Singer, Maple, and Bowen [15, 16] and by Cahill, Jr.,[14] indicate the existence of electric currents at 100-110 km above the geomagnetic equator. Thus it is clearly established that the E-region of the ionosphere is the main conducting region or the dynamo layer.

Fields and Currents in the Ionosphere

The electric fields and electric currents in the dynamo layer resulting from lunar tides are derivable by the application of the revised dynamo theory to a semidiurnal tidal wind-velocity potential that is independent of height and has the form

$$\psi = ka \sin^2\theta \sin 2\phi, \qquad (1)$$

where k is an amplitude coefficient, a the radius of the dynamo layer, θ the geomagnetic colatitude, and ϕ an abbreviation for $t + \lambda + \alpha$, in which t is the

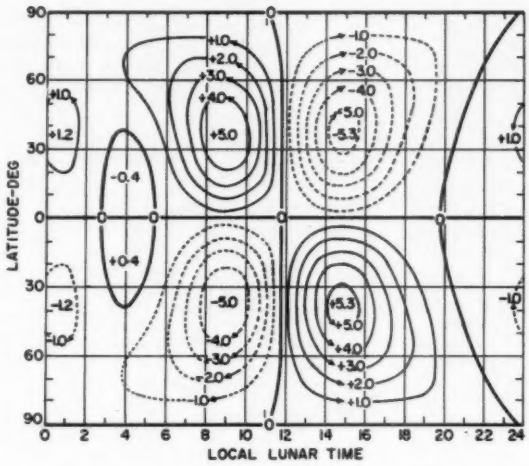

FIG. 3. CURRENT SYSTEMS AT THE EQUINOXES THAT COULD PRODUCE NEW-MOON DAILY VARIATIONS

Greenwich time in angular measure, λ the longitude, and α a phase constant. However, the electric fields and currents obtainable in this way could only be expressed in relative magnitudes, since the value of k has never been estimated theoretically. This constant can be evaluated by making use of the upper-atmospheric current systems deduced by Chapman and Bartels[17] from the daily magnetic variations. A brief digression about the representation of these current systems is instructive.

The current systems of Chapman and Bartels may be regarded as a world view of the relative intensities of the daily magnetic variations at different seasons and latitudes and, in the case of lunar magnetic variations, at different phases of the moon. Figure 3 depicts the current system responsible for the lunar daily magnetic variation on a new-moon day during the solar equinoxes. The currents flow in four closed circuits in the sunlit hemisphere, the intensity of each being about 5300 amperes. In the night hemisphere they flow in two circuits, one to the north and the other to the south of the equator, the intensity of each being about 1200 amperes. This difference between night and day currents conforms with the observed larger lunar magnetic variations during daylight hours than during the night. Figure 4 represents the mean for a lunar month, during the solar equinoxes. Since during a whole lunar month the daylight hours are equally distributed over all parts of the lunar day, this current system consists of eight closed circuits, symmetrically spaced, the current in each being about 2600 amperes.

Even though the Chapman and Bartels' current systems were deduced from the daily lunar magnetic variations, it was found later that they do not fit the

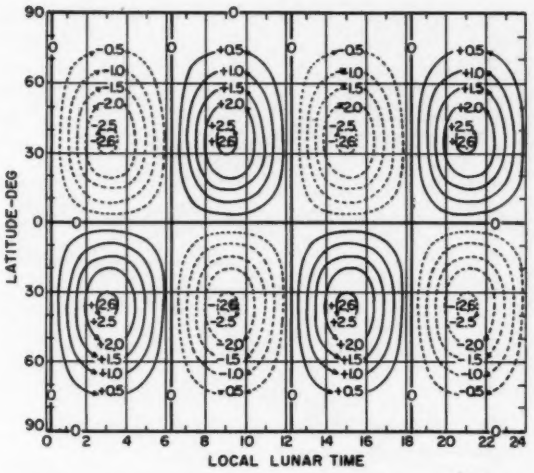

FIG. 4. CURRENT SYSTEMS AT THE EQUINOXES THAT COULD PRODUCE MONTHLY MEAN DAILY VARIATIONS

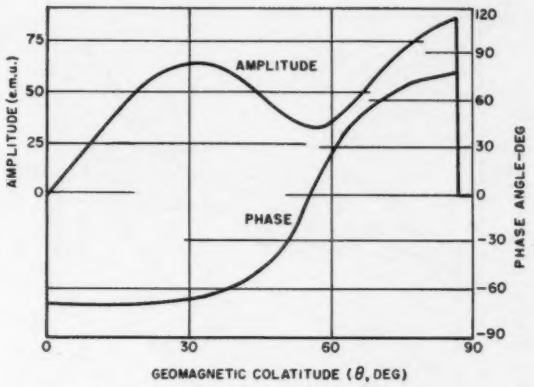

FIG. 5. THE TOTAL SOUTHWARD ELECTRIC FIELD

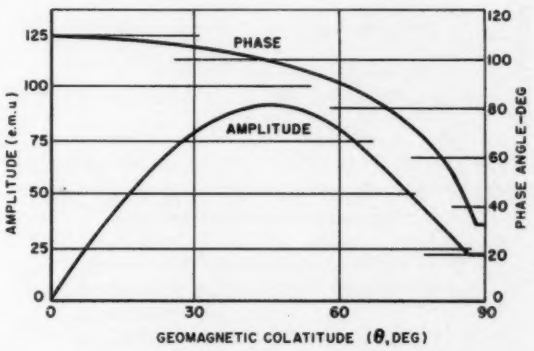

FIG. 6. THE TOTAL EASTWARD ELECTRIC FIELD

enhanced magnetic variations near the geomagnetic equator. The revised dynamo theory, however, takes care of these equatorial enhancements. A comparison of the nonequatorial latitudinal variation of the Chapman and Bartels' current systems with those derived by the application of the revised dynamo theory leads to the evaluation of the unknown amplitude coefficient, k. Thus the absolute magnitudes of the electric fields in the dynamo layer are those represented in Figs. 5 and 6. Positive phase angles in these plots correspond to leads, from the lunar transit, at the rate of 30° per one hour. As can be seen, the southward electric field reverses its phase at about 35° latitude.

As mentioned earlier, these electric fields in the dynamo layer are a sum of the dynamo or induced fields and the polarization fields. The polarization fields are coupled from the dynamo region to other regions along the equipotential geomagnetic field lines. Thus, although these fields are generated in the dynamo layer, they affect other regions as well. To estimate the effect of the polarization fields on the other layers, one should know what portion of the total electric field in the dynamo layer is due to polarization. Conductivity calculations and other relevent considerations indicate that in the equatorial strip the entire field is due to polarization, whereas in the rest of the region about 80% of the total electric field is due to polarization.

VERTICAL IONIC DRIFT

In the ionosphere, which is considered as a series of thin spherical conducting shells, the magnetic field is inclined to the surface of the shells. The electric fields and currents, which are essentially in the plane of the ionosphere, cause a drift of neutral ionization. This drift is perpendicular to both the direction of current and the direction of the magnetic field, and necessarily has both horizontal and vertical components. This study, however, is concerned only with the vertical drift velocities, v, which are related to the electric fields by a formula of the type

$$v = r_1 \frac{E_y}{H} - r_2 \frac{E_x}{H}, \qquad (2)$$

where E_x and E_y are the southward and eastward electric fields in the region under investigation, r_1 and r_2 are quantities into which the height distribution of electron density and conductivity are lumped, and H is the intensity of the earth's magnetic field. The results of such a calculation are plotted in Figs. 7 and 8.

Figure 7 indicates the amplitudes of the vertical ionization-drift velocities, due to the lunar semidiurnal tide, at various heights ranging from 90 km to 300 km. Figure 8 represents the phases, in hours after lunar transit, of these velocities. As is at once apparent, at E-region heights the amplitude of drift

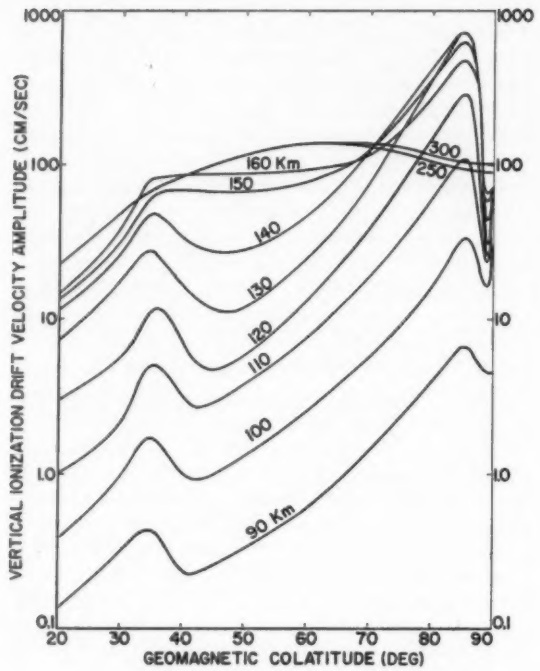

FIG. 7. VERTICAL IONIZATION-DRIFT VELOCITY AMPLITUDE VS GEOMAGNETIC COLATITUDE

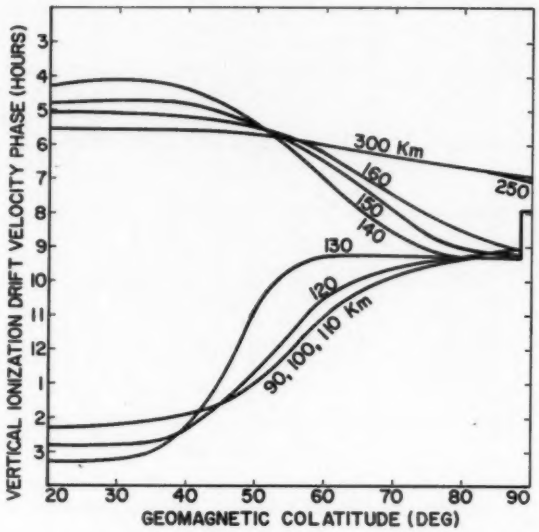

FIG. 8. VERTICAL IONIZATION-DRIFT VELOCITY PHASE VS GEOMAGNETIC COLATITUDE

velocity is large in the vicinity of the magnetic equator and small beyond about 30° of geomagnetic latitude. A gradual change in the phase of the velocity, from about 8 hours after lunar transit near the equator to about 14 hours (equivalent to 2 hours) after lunar transit near the poles, occurs around geomagnetic latitude 35°. As can also be seen, the vertical ionization-drift velocity has a large height gradient at these heights. However, at F_2-region heights the latitudinal variation of drift-velocity amplitudes is not so marked. The change in phase of v is only about 1.5 hours, from 7 hours after lunar transit near the geomagnetic equator to about 5.5 hours after lunar transit near the poles. The height gradient of v is also negligible in this region.

It follows immediately that the next step in this treatment is to investigate the consequences of this vertical ionic drift on the F_2 and the E ionospheric layers. In this step the other processes in the ionosphere, such as electron production, electron loss, and diffusion, have also to be taken into account, and the combined effects of these and the tidal drift must be determined. These are necessary considerations because the experimental results of the lunar variations contain the effects of all these processes. A comparison of experimental results with these theoretical results is then appropriate.

F_2-LAYER VARIATIONS

A full-fledged investigation without an approximation to the height distribution of the ionospheric processes just mentioned is very hard to accomplish. Hence the following approximate expression for the velocity, W, of vertical movement of h_mF_2, the height of maximum ionization of the F_2 layer, will be employed:

$$W = -ae^{-z} + be^{-z} - ce^{z} + v. \qquad (3)$$

Into this expression are lumped the effects due to electron production, electron loss, diffusion, and tidal drift, which are represented by a, b, c, and v. The factors $e^{\pm z}$ take care of the height variations. Since the height gradient of v is negligible at F_2-region heights, no such factor is attached to this term. Since the electron production is due to solar radiation, the factor a becomes zero during night, whereas during daytime it dominates. The diffusion term has negligible influence during daytime. As a result, the effect of the tidal drift has to be calculated separately for day and night, taking into account the light-to-darkness inequality of the current systems and hence the drift velocities. In both the cases, the drift velocity produces only these perturbations:

Δh_mF_2, in the height of maximum ionization density, and

ΔN_mF_2, in the value of maximum electron density.

The method of estimating Δh_mF_2 consists of first setting $v = o$ in the expression for W and calculating the equilibrium height of the layer, and then

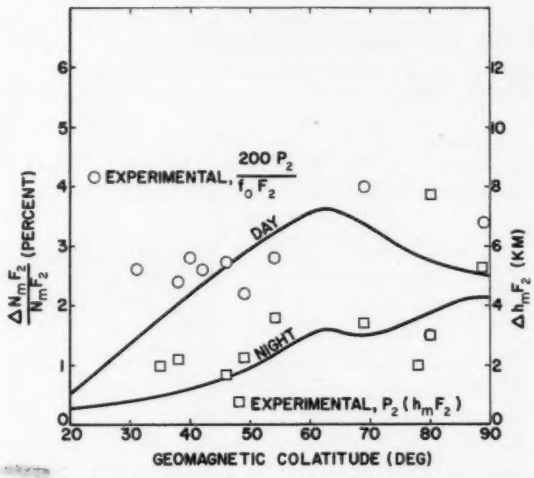

FIG. 9. AMPLITUDE OF SEMIDIURNAL LUNAR VARIATIONS in b_mF_2 and N_mF_2

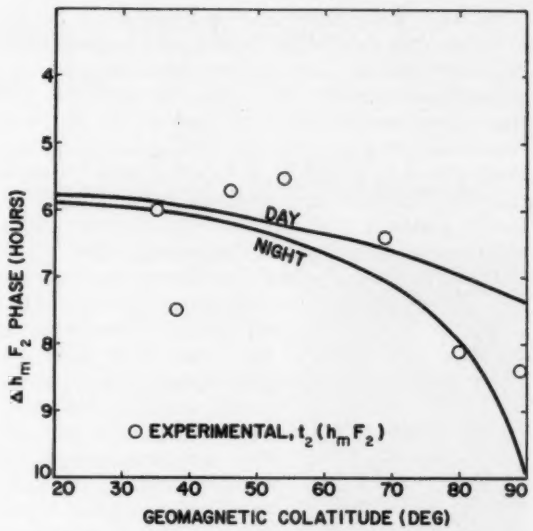

FIG. 10. PHASE OF SEMIDIURNAL LUNAR VARIATIONS in b_mF_2

determining the new equilibrium height with a value assigned for v. The difference in the two equilibrium heights will then be equal to the amplitude of Δh_mF_2. The phase lag of Δh_mF_2 over the drift velocity is equal to half of the amplitude of Δh_mF_2 divided by the amplitude of the drift velocity. The perturbation in the maximum electron density, expressed as fraction of the maximum electron density, can then be evaluated from the expression

$$\frac{\Delta N_mF_2}{N_mF_2} = \frac{\beta \Delta h_mF_2}{H_o\sqrt{4\omega^2+\beta^2}}\,; \qquad (4)$$

and it lags the perturbation in h_mF_2, by an angle ϕ, given by

$$\phi = \arctan\frac{2\omega}{\beta}\,, \qquad (5)$$

where β is a coefficient representing electron decay, ω is the angular velocity of the earth's rotation, and H_o, the scale height of the F_2 layer.

Assuming the most reliable values [18, 19, 20] available thus far for the F_2-region parameters, the perturbations Δh_mF_2 and $\frac{\Delta N_mF_2}{N_mF_2}$ are calculated as a function of geomagnetic colatitude for both day and night conditions. The solid curves in Fig. 9 represent these calculated values of amplitudes of Δh_mF_2 and $\frac{\Delta N_mF_2}{N_mF_2}$, to different scales. The latter is expressed as a percentage so as to compare it with the experimentally available $\frac{200P_2}{f_oF_2}$. The solid curves in Fig. 10 represent the calculated phase values of Δh_mF_2. The perturbation in the maximum electron density lags Δh_mF_2 by constant amounts of two hours during the day and three hours during the night. To compare these theoretical results, the corresponding experimental results obtained from Table I are plotted in the respective figures. From these, it can be easily inferred that there is, in general, a good agreement between the theoretically obtained results and the experimentally deduced values.

E-LAYER VARIATIONS

Now it will be interesting to investigate whether the same general agreement exists for the E-layer variations. For this case, the only experimentally available results are the lunar semidiurnal variations in $h'E$ (and E_s), both in amplitude and phase. Hence, for comparison, the effect of vertical ionic-drift velocity on the minimum equivalent height of the E layer has to be evaluated. However, this evaluation, which requires a computer, is probably not worth while at this time since many of the experimental results are questionable, as will be indicated later. On the other hand, the perturbation, Δh_mE, in the height of maximum ionization density of E layer is easier to calculate by using an approximate expression, derived by Appleton and Lyon[21],

$$\Delta h_mE = \frac{v}{2\alpha N_m}\,, \qquad (6)$$

where α is a coefficient representing electron decay and N_m is the maximum electron density. As can be seen from this expression, the height gradient of drift velocity does not affect Δh_mE. It should also be pointed out that diffusion has negligible importance in the E region and so was not considered in deriving the above expression.

After the values of Mitra[20] and Appleton[22] for the E-region parameters are chosen, the amplitudes of $\Delta h_m E$ for both day and night are computed at selected geomagnetic latitudes. The phases of $\Delta h_m E$ are obtained in a manner similar to those of $\Delta h_m F_2$. The results are presented in Table III. A comparison of these with the corresponding experimentally obtained results of $h'E$ (and E_s) variations, given in Table II, clearly indicates a discrepancy between the theory and experiment, in both amplitude and phase.

The calculated amplitude variations from theory are high at low latitudes and very low at high latitudes, whereas the experimental results show an exactly opposite trend. The phase reversal of the lunar variations at about geomagnetic latitude 35° is not evident in the experimental results, perhaps because most of these are for locations above geomagnetic latitude 35°. Even then, the phases seem to be scattered around 6 to 10 hours, whereas according to theory the maximum lunar variations at these latitudes should occur at about 0.5 to 2 hours after lunar transit. These discrepancies may be attributed to the following reasons:

1. The published values of the minimum equivalent height, $h'E$ (and E_s) of the E (and E_s) layer, from which the experimental results are deduced, have a very limited accuracy. Moreover, the experimental work at different locations was done at widely separated intervals of time, so that the results lack consistency. This is more apparent because the results for the same location, but at different periods, show considerable divergence.

2. For more accurate comparison between theory and experiment, the experimental results must be deduced from an analysis of actual heights rather than virtual heights. None of the available experimental results are obtained in this manner.

3. In the theoretical treatment, the semidiurnal lunar-tidal wind has been assumed to be uniform with height in the dynamo layer. But actually it may have some height gradient, which cannot possibly be estimated from the presently available information. However, this can only slightly change the amplitudes of the variations derived from theory, and it does not affect their latitudinal distribution.

4. Most of the available E-region experimental results shown in Table II are obtained from the sporadic E-layer data. According to one version of the causes of sporadic E ionization, irregularities in electron density distribution are formed in this region. Local polarization fields may be established at these irregularities; and these polarization fields might change the total electric fields derivable from the revised dynamo theory, and hence might contribute to the disagreement between the theoretical and experimental results.

TABLE III

CALCULATED VALUES OF $\Delta h_m E$ AT DIFFERENT GEOMAGNETIC LATITUDES

GEOMAGNETIC LATITUDE	DAY		NIGHT	
	AMPLITUDE (km)	PHASE (hr)	AMPLITUDE (km)	PHASE (hr)
1°	0.17	8.00	0.60	8.70
10°	1.00	9.30	3.45	10.00
36°	0.07	0.25	0.21	0.95
44°	0.03	1.45	0.11	2.15
56°	0.07	2.10	0.23	2.80

In conclusion, we can say that the calculated semidiurnal lunar variations in the height of maximum ionization density and in the maximum ionization density of the F_2 region agree well with those derived from the experimental data for the ionospheric F_2 region. But more research is needed before we can resolve the discrepancy between the calculated semidiurnal lunar variations in the height of maximum ionization density of the E region and those variations in $h'E$ (and E_s) derived from the experimental data for the ionospheric E (and E_s) layer.

REFERENCES

1. SWARM, H. M., DOBROTT, D. R., and NAGATA, R., "Lunar Tidal Variations in the Height of Ionospheric Layers," *The Trend in Engineering at the University of Washington*, Vol. 10, No. 3, July, 1958, p. 8.
2. BOOKER, H. G., and SEATON, S. L., "Relation between Actual and Virtual Ionospheric Height," *Assoc. Terr. Mag. and Elect. Bulletin*, Vol. 11, 1940, p. 503.
3. STEWART, B., *Encyclopedia Britannica*, 9th ed., 1882.
4. SCHUSTER, A., "The Diurnal Variation of Terrestrial Magnetism," *Phil. Trans. Roy. Soc.*, A, Vol. 208, 1908, p. 163.
5. CHAPMAN, S., "The Solar and Lunar Diurnal Variations of Terrestrial Magnetism," *Phil. Trans. Roy Soc.*, A., Vol. 218, 1919, p. 1.
6. TAYLOR, G. I., "The Oscillation of the Atmosphere," *Proc. Roy. Soc.*, A., Vol. 156, 1936, p. 318.
7. PEKERIS, C. L., "Atmospheric Oscillations," *Proc. Roy. Soc.*, A., Vol. 158, 1937, p. 650.
8. COWLING, T. G., "The Electrical Conductivity of an Ionized Gas in the Presence of a Magnetic Field," *Mon. Not. R. Astr. Soc.*, Vol. 93, 1933, p. 90.
9. BAKER, W. G., and MARTYN, D. F., "Electrical Currents in the Ionosphere, I," *Phil. Trans. Roy Soc.*, A, Vol. 246, 1954, p. 281.
10. BAKER, W. G., "Electrical Currents in the Ionosphere, II," *Phil. Trans. Roy. Soc.*, A., Vol. 246, 1954, p. 295.
11. MARTYN, D. F., "Electrical Currents in the Ionosphere, III," *Phil. Trans. Roy. Soc.*, A., Vol. 246, 1954, p. 306.
12. HIRONO, M., *Jour. Geomag. Geoelec. Kyoto.*, Vol. 2, 1950, p. 1.
13. FEJER, J. A., "Semidiurnal Electron Currents and Drifts in the Ionosphere," *J. Atmos. & Terr. Phy.*, Vol. 4, 1953, p. 184.
14. CAHILL, Jr., L. J., "Investigation of Equatorial Electro-Jet by Rocket Magnetometer," *J. Geophy. Research*, Vol. 64, 1959, p. 489.
15. SINGER, S. F., *et al*, "Evidence for Ionospheric Currents from Rocket Experiments near the Geomagnetic Equator," *J.Geophys. Research*, Vol. 56, 1951, p. 265.

(Continued on page 30)

The Implications of Isentropic Nozzle Flow for a Perfect Gas

CHARLES P. COSTELLO
Assistant Professor of Mechanical Engineering

WILLIAM B. NORDQIST
Associate Professor of Mechanical Engineering

C. P. Costello

The authors have long been concerned with the fact that a basic relation of classical thermodynamics has always been used in an application that apparently does not satisfy the requirements imposed on the basic relation. The problem in question concerns flow in a nozzle at constant entropy (isentropic flow), a problem that appears in a tremendous number of thermodynamic analyses.

To determine exact relations among the thermodynamic properties of the flowing fluid, we made an analysis of frictionless adiabatic flow of a Perfect Gas in a nozzle. We found that the relations commonly employed in classical thermodynamics are valid, although the relations are based on an equation not strictly applicable in the case analyzed. Our investigation also shows that there is a single nozzle design to provide true frictionless, adiabatic flow rather than a family of nozzles as is implied by standard works on the subject. In this article we present a straightforward approach for obtaining the relations among properties that must hold for flow of fluids, even for the ones that cannot be considered Perfect Gases.

Nature of the Problem

The entropy function of a system, as defined in classical thermodynamics, is

$$ds = \left(\frac{dQ}{T}\right)_{Reversible} \qquad (1)$$

where s = entropy, Q = heat transfer to the system in question, T = absolute temperature at which heat transfer takes place, and *Reversible* signifies that the system in question must be in complete equilibrium with its surroundings and within itself.

A nozzle, a device used to transform energy available in other forms to kinetic energy, is widely used. In nozzles the heat transfer to or from the surroundings is usually an extremely small quantity. Since *reversible flow* implies ideal frictionless flow and also implies that all possible energy available in other forms is transformed to kinetic energy, *reversible flows* are highly desirable. As an ideal for nozzle design, then, a reversible and adiabatic model is commonly considered, *adiabatic* signifying no heat transfer. The stipulations of adiabatic reversible behavior require that the entropy be a constant $ds = O$, by the definition of the entropy function just given in Eq. (1).

W. B. Nordquist

In classical thermodynamics the nozzle is analyzed on the basis of isentropic behavior. In order to solve for the kinetic energy at the nozzle outlet in terms of pressure drop across the nozzle, a requirement is to have some relation among the properties of the fluid flowing through the nozzle. The problem of evaluating exit kinetic energy becomes very elementary once some relation among properties is derived that holds throughout the length of the nozzle.

It seems possible to arrive at just such a relation if constant entropy flow is assumed and the flowing fluid is treated as a Perfect Gas. The Gibbs' relation from classical thermodynamics is, in part,

$$ds = \frac{du}{T} + \frac{P dv}{T}, \qquad (2)$$

where T = absolute temperature, u = internal thermal energy, P = pressure, and v = specific volume.

This relation holds for a unit mass of a pure fluid substance not subjected to external fields. For the equation to hold, there must be no appreciable internal movement of a portion of the mass relative to the center of gravity of the mass, although the center of gravity itself may move. If such relative movement is present or if external fields are influential, terms must be added to Eq. (2) to account for these factors. In the usual analysis of nozzle flow, it is assumed at the outset that such factors are inconsequential, and Eq. (2) is employed.

For a Perfect Gas, one that obeys the equation

$$Pv = \frac{RT}{m}; \qquad (3)$$

NOMENCLATURE

A = cross-sectional area for flow, ft²

C = constant, defined by Eq. 8, ft − °F

C_p = specific heat at constant pressure, ft-lb$_f$/lb °F

C_v = specific heat at constant volume, ft-lb$_f$/lb °F

g_c = constant of proportionality in Newton's Second Law, lb/lb$_f$ ft/sec²

h = enthalpy of fluid, ft-lb$_f$/lb

K = thermal conductivity, lb$_f$/hr °F

k = ratio, C_p/C_v, dimensionless

M = mass rate of flow, lb/sec

m = molecular mass of fluid, lb/lb mol

P = pressure, lb$_f$/ft²

Q = heat transfer, ft-lb$_f$

R = universal gas constant, ft-lb$_f$/lb mol °R

°R = signifies degrees Rankine, absolute temperature

s = entropy function, ft-lb$_f$/lb °R

T = temperature, °R

u = internal thermal energy of fluid, ft-lb$_f$/lb

V = velocity of flow in X direction, ft/sec

x = directional coordinate, ft

v = specific volume, ft³/lb

---

where R = universal gas constant and m = molecular mass of the substance, it may be shown that

$$du = C_v dT. \tag{4}$$

The specific heat at constant volume, C_v, is a constant for the Perfect Gas. Combining (2), (3), and (4) with the assumption that the flow is at constant entropy, we obtain for the fluid as a system

$$O = \frac{c_v dT}{T} + \frac{R}{m}\frac{dv}{v}. \tag{5}$$

This is an exact differential equation that may be integrated between any two states achieved by the flowing fluid. This provides the necessary relation among the fluid properties anywhere along the nozzle. The result of the integration, when combined with (3), is

$$Pv^k = \text{(constant) anywhere along a nozzle,} \tag{6}$$

where $k = \frac{Cp}{C_v}$, a constant for the Perfect Gas, and Cp = specific heat at constant pressure, a constant for the ideal gas. Equation (6) is invariably used in the preliminary design of nozzles, to arrive eventually at a value for the exit kinetic energy of the fluid in terms of the pressure drop from entrance to exit of the nozzle.

The nature of the dilemma we now face is this: As explained above, Eq. (2) is valid for a fluid only in the absence of motion within the fluid itself. Since Eq. (6) is derived from Eq. (2), Eq. (6) is also invalid if the fluid itself has any motion within it. Clearly, in a nozzle there is a change in the amount of kinetic energy stored within the *fluid itself* because individual portions of the fluid must continuously accommodate themselves to the converging or diverging walls of the nozzle passage. Seemingly, then, the Gibbs' Eq. (2) should be modified to account for motion within the system itself by adding additional terms. The nature of velocity variations within the system will now be discussed at some length, since their exact nature is important.

As we must emphasize, the velocity that would affect Eq. (2) is not all of the velocity a stationary observer would see when looking at the unit mass of a substance flowing through a nozzle. Equation (2) is still valid in accelerating systems, provided an observer riding along with the center of gravity of the system observes no motion; that is, the motion that has to be excluded so as to use Eq. (2) is the motion of one portion of the system relative to another and not that of the center of gravity of the system. But in the nozzle flow we obviously have the former class of motion: an observer riding on the center of gravity of a unit mass flowing through a nozzle would observe portions of the system converging on him or diverging from him. Nor does it seem safe to neglect this motion as being negligible *a priori*; intuition tells us that such velocities have considerable magnitude in large nozzles with high flow rates.

Certainly there must be motion of one portion of the unit mass flowing through a nozzle relative to the boundaries of its own system: without it the fluid could not accommodate to the passage walls. If continuity is to be maintained, the system must also expand in the direction of flow relative to its own center of gravity. The analysis to be presented will be primarily concerned with this second kind (expansion of the system in the flow direction), although both types of motion relative to the system's own center of gravity are actually accounted for. The velocity in the x direction will be denoted by V, and the velocities normal to the x direction are actually considered as part of the internal thermal energy of the fluid. This is permissible within the system to be defined since, under the circumstances involved here, internal energy and transverse molecular velocities are equivalent.

How much will these motions internal to the system alter Eq. (6)? We set out to answer this ques-

tion by using neither Eq. (2) nor (6) and arrived at remarkable results and an insight into aspects of isentropic nozzle flow for a Perfect Gas. In passing along this insight, the authors need to present their analysis of this intriguing problem.

Fundamental Approach to the Problem

The problem may be restated in this way: given a perfect gas, flowing steadily, reversibly, and adiabatically in a rigid insulated nozzle, what is the relation among properties that must hold continuously along the nozzle to ensure such isentropic flow?

The control-volume approach will be used. That is, fixed imaginary boundaries will be set up, separated by distance dx, and flow will be allowed to enter and leave these boundaries. Property values of the fluid and characteristics of the system are shown in Fig. 1.

No Net Heat Transfer. While no heat transfer from the surroundings is permitted (because of the specification that the nozzle is insulated), fulfilling the requirement of adiabatic flow makes necessary the assurance that no heat is transferred by conduction through the fluid itself. This is accomplished by writing

$$-KA\,\frac{dt}{dx}=-\left[K(A+dA)\left(\frac{dT}{dx}+\frac{d^2T}{dx^2}\,dx\right)\right], \qquad (7)$$

where K is the thermal conductivity, assured constant; A is the cross-sectional area for flow; T is the temperature; and x is the length coordinate. The left side of Eq. (7) is heat inflow by conduction, the right side heat outflow by conduction. The solution to Eq. (7) that guarantees adiabatic behavior is

$$\frac{dT}{dx}=\frac{C}{A}, \qquad (8)$$

where C is a constant.

Conservation of Energy. For the system shown in Fig. 1, energy is conserved if the equation

$$O=dh+d\left(\frac{V^2}{2g_c}\right) \qquad (9)$$

is satisfied, because we have already removed all possibilities of net heat transfer. In this equation h is the enthalpy of the fluid, V is the absolute fluid velocity, and g_c is the constant of proportionality in Newton's Second Law. The enthalpy accounts for the internal thermal energy of the system and the flow work done in crossing the system boundaries; V is the velocity observed by a stationary observer, and, as pointed out above, part of this velocity is due to

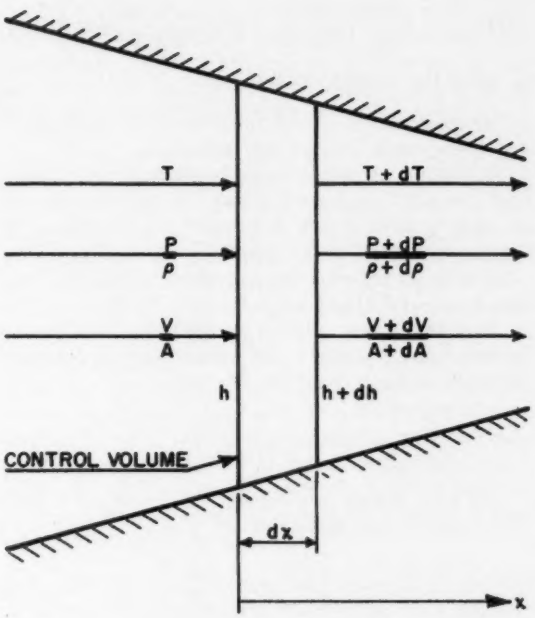

FIG. 1. INSULATED NOZZLE FOR CONSTANT ENTROPY FLOW

motion of the system center of gravity, which in itself would not preclude use of Eq. (2). But since portions of V may be due to velocities of the fluid relative to its own center of gravity, we will not employ Eq. (2) for the sake of complete generality.

Continuity Equation. Since the mass rate of flow, M. is to be a constant in the nozzle, continuity requires

$$M=\frac{AV}{v}. \qquad (10)$$

By differentiation it may be established that

$$VdV=\frac{M^2}{g_cA^2}\left[vdv+v\frac{dA}{A}\right] \qquad (11)$$

at any point in the nozzle. Combined with Eq. (9) this yields

$$O=dh+\frac{M^2v}{g_cA^2}\left[dv-v\frac{dA}{A}\right] \qquad (12)$$

Equation (8) may be differentiated to yield

$$\frac{dA}{A}=\left[\frac{d^2T/dx^2}{dT/dx}\right]dx \qquad (13)$$

and, by combining (12) and (13),

$$O=dh+\frac{M^2\nu}{C^2g_c}\left(\frac{dT}{dx}\right)^2\left[d\nu+\nu\frac{d^2T/dx^2}{dT/dx}dx\right], \quad (14)$$

C being the constant of Eq. (8).

Momentum. To satisfy the momentum equation for the control volume, we write:

(Force on left of the control volume in the x direction) $= (PA + PdA)$, where dA accounts for the element of area in the x direction at the top of the stationary control volume, and

(Force on right of control volume in the x direction) $= -(P + dP)\ (A + dA)$.

The net force, AdP, (neglecting higher-order terms) must be equal to the change of momentum of the fluid in the x direction, or

$$-AdP=\frac{MdV}{g_c}. \quad (15)$$

We now employ the Perfect Gas equation of state (3), which when differentiated yields

$$dP=\frac{R}{m}\left[\frac{1}{\nu}dT-\frac{Td\nu}{\nu^2}\right]. \quad (16)$$

By combining (16), (8), and (10) and by differentiating the latter two equations to obtain relations for dA and dV respectively, we get by tedious algebra

$$\frac{C}{dT/dx}\frac{R}{m\nu}\left[dT-\frac{Td\nu}{\nu}\right]$$

$$=\frac{-M^2}{Cg_c}\left[\frac{dT}{dx}d\nu+\nu\frac{d^2T}{dx^2}dx\right]. \quad (17)$$

The constant, C, is that of Eq. (8).

Equation (17) provides a means of obtaining a value for the constant, C, in terms of properties of the fluid. This is necessary to complete the problem because C also appears in Eq. (14), which was derived from energy and continuity requirements. The constant C must be eliminated in order to arrive at a relation among properties. Equation (17) yields

$$C^2=\frac{M^2m\nu}{g_cR}\frac{dT}{dx}\left[\frac{\frac{dT}{dx}d\nu+\nu\frac{d^2T}{dx^2}dx}{\frac{Td\nu}{\nu}-dT}\right] \quad (18)$$

Enthalpy for a Perfect Gas. To attempt to evaluate properties of the fluid in terms of conditions that are usually known, we must express *enthalpy* in terms of easily measured properties. The definition of enthalpy is

$$h=u+P\nu, \quad (19)$$

which is equivalent to

$$h=u+\frac{RT}{m} \quad (20)$$

for a Perfect Gas.

On a microscopic level, internal thermal energy depends on the kinetic energy of molecules. It is the kinetic energy of the molecules that manifests itself as what is commonly called temperature. If pressure, volume, or other properties of the system are capable of causing interaction among molecules, internal thermal energy will be in part determined by such properties. In all real substances this is the case, and internal thermal energy is a function of temperature and some other variable, say pressure. In the idealized Perfect Gas, this is not so. Any idealized substance that obeys the Perfect Gas Law (3) *ipso facto* has no intermolecular forces; in such cases, internal thermal energy is a function solely of temperatures. This concept is commonly used for Perfect Gases, but the proof usually rests on an assumption that a relation like (2) holds. We wish to keep the relations used here perfectly general. We postulate, then, that internal thermal energy is a function of temperature only. The equipartition of the energy theorem of kinetic theory* bears out this contention.

Equation (20), then, states that enthalpy is also a function only of temperature for a perfect gas. The relation of enthalpy to temperature is

$$dh=C_pdT, \quad (21)$$

where C_p is the specific heat at constant pressure.

Summary of Computing Equations

We will now substitute (18) and (21) into (14) and collect the important equations used to date. The substitution results in

$$O=C_pdT+\frac{R}{m}\left(\frac{dT}{dx}\right)\left[\frac{\frac{T}{\nu}(d\nu)^2-dTd\nu+T\left(\frac{d^2T/dx^2}{dT/dx}\right)d\nu dx-\frac{d^2T/dx^2}{dT/dx}\nu dTdx}{\frac{dT}{dx}d\nu+\nu\frac{d^2T}{dx^2}dx}\right] \quad (22)$$

Also we have previously used

$$M=\frac{AV}{\nu} \quad \text{(continuity)}, \quad (10)$$

$$\frac{dT}{dx}=\frac{C}{A} \quad \text{(to eliminate conduction-heat transfer)} \quad (8)$$

* *Introduction to Modern Physics*, Richtmeyer, Kennard, and Lauritsen, 5th ed., (McGraw-Hill) New York, 1955, 119.

$$Pv = \frac{RT}{m} \quad \text{(Perfect Gas)}, \tag{3}$$

$$O = C_p dT + \frac{M^2 v}{g_c A^2}\left[dv - \frac{v dA}{A}\right] \quad \text{(energy and continuity Plus Eq. 21)}, \tag{23}$$

and

$$C^2 = \frac{M^2 mv}{g_c R}\frac{dT}{dx}\left[\frac{\frac{dT}{dx}dv + v\frac{d^2T}{dx^2}dx}{\frac{T}{v}dv - dT}\right]$$

(from momentum, continuity, Perfect Gas, and conduction). (18)

By use of the equations above, we have ensured adiabatic behavior. We have also ensured that the flow will be frictionless and that each lamina of the fluid will be in equilibrium within itself and with its surroundings. This has been ensured by eliminating frictional forces in the momentum equation and by writing unique values of properties for the lamina of fluid. The latter practice requires that the fluid be in internal equilibrium; and by writing only differential property changes we have specified that the system is in equilibrium with its surroundings as well.

Since the flow is reversible and adiabatic, the entropy is constant by definition (1). The question remains, what relation among properties must hold along the length, x, in order that all of the equations listed above are satisfied?

Obviously boundary conditions will enter this problem. These need only be specification of a mass rate of flow, pressure drop across the nozzle, and conditions at the nozzle entrance, conditions that are normally known to the designer. Then the equations, when satisfied, will give the nozzle area and fluid temperature, specific volume, and other properties, all as a function of x. These variations with x will be the ones required to assure isentropic flow.

Upon arriving at the equations summarized above, the authors were prepared to eliminate the ruinous *a priori* assumption of Eq. 6. They planned to work out a finite-differences solution by employing a digital computer; but they discovered that Eq. 6 is, in fact, the only possible relation that permits simultaneous satisfaction of all of the equations. It is remarkable that such a simple specification satisfies specifications on equations of state, continuity, momentum, heat transfer, and overall energy balances.

Implications of Isentropic Flow of a Perfect Gas

The requirements that must be satisfied for a Perfect Gas to undergo isentropic flow are as follows:

1. The energy owing to expansion of portions of the unit mass of a Perfect Gas relative to its own center of gravity must be negligible. This is absolutely true, since any finite effect of such expansion would invalidate Eq. (6), which does actually satisfy all of the equations that must hold for isentropic flow.

2. For a Perfect Gas, there is a unique nozzle that guarantees isentropic flow for each condition of mass-flow rate, pressure drop across the nozzle, and fluid properties at the inlet. The area as a function of x may be obtained from the foregoing equations that contain A and x factors. Usually, it is implied that a family of nozzles exists to give isentropic flow with a specified pressure drop across the nozzle. Strictly speaking, this is not so. The unique area requirement is derived from Eq. (7), which is based on the requirement that conduction-heat transfer must be zero. This is neglected generally because the conduction-heat transfer is considered negligible *a priori*. However, the equations we have listed enable the construction of a nozzle ensuring the absence of heat transfer by conduction.

3. Finally, and perhaps most important, we can write a system of equations ensuring flow at constant entropy (reversible adiabatic flow) without resort to such relations as (2). A system of these equations may be solved by trial and error to obtain a continuous relation among properties of the fluid in question. In the particular case of a Perfect Gas the equations are satisfied by (6). For substances other than Perfect Gases, the approach would differ only slightly. If a more complex equation of state than Eq. (3) is used to describe a fluid, a property relation different from (6) would result, but the procedures employed in arriving at the result would not be markedly different from those employed here. We can safely say, however, that the result would be derived only at the expense of considerable labor, and that the problem should be programmed for a trial-and-error solution on a digital computer.

STRAWS IN THE WIND

An engineering degree is no longer a passport to a good job? This is the opinion of the Office of Student Personnel of the Cornell University College of Engineering. Because of the intense competition for engineering graduates that developed a few years ago, many companies have been hiring liberal arts graduates and technicians to fill jobs previously held by engineers. Cornell also reports that its five-year curriculum is paying dividends to its graduates in the form of higher-than-average starting salaries. *Civil Engineering*, Vol. 30, No. 3, March, 1960.

Engineering Research Dividends

Recent theses submitted for advanced degrees from the College of Engineering, University of Washington, will regularly appear in abstract form in *The Trend*. Complete copies of these theses are available for reference at the University of Washington Library. Address inquiries to the Director of the Engineering Experiment Station, University of Washington, Seattle 5.

CRUMBLEY, D. L., "A Study of Fuel Consumption and Travel Time Characteristics of Diesel Powered Vehicles," M.S. in Civil Engineering, 1960.

This thesis is divided into two parts: Part A, which is a report of the seasonal effect on fuel consumption of diesel-powered vehicles; and Part B, which includes the identification and use of some of the more easily measured variables used to estimate travel time and enroute fuel consumption.

In the section devoted to seasonal effect on fuel consumption, a large part of the field work proved to be inadequate due to the malfunctioning of the basic metering unit. Therefore, alternate sources of information were used as a basis for this portion. Primarily these sources were various trucking companies' records and local climatological reports. Data obtained from a controlled test vehicle was used to make a spot check of the accuracy of the trucking records.

The second portion of this paper includes the identification and use of rise, fall, weight, horsepower, and distance to estimate travel time and enroute fuel consumption. These empirical variables were selected and equated to form two families of curves, one for estimation of enroute fuel consumption and the other for estimation of travel time.

The facts learned by this investigation could be applied with significance to the field of highway economics and for economic transport-route feasibility calculations for the trucking industry.

LARSON, J. R., "Boundary Layer Transition in Natural Convection," M.S. in Engineering, 1960.

The transition of laminar to turbulent flow in a natural-convection boundary layer was experimentally studied to determine if the transition might be correlated as a function of the Grashof number or Grashof-Prandtl number product. To accomplish this, a test apparatus consisting of a vertical copper pipe heated internally by electrical resistance wiring was submerged in a test fluid of water or ethylene glycol. The temperature of the ambient fluid and the copper-pipe surface was kept nearly constant for a test run. The fluids were picked so that by varying their temperature the Prandtl number could be varied from two or three for water to over 100 for ethylene glycol.

The sine-shaped wave of the initial instability leading to transition and turbulent flow was visually observed by means of a concentrated arc light that projected parallel light by the vertical edge of the pipe. Flash glass or a wall served as a screen for the image of the boundary layer. The lowest point on the cylinder at which instability occurred was noted and measured to within about ¼ in. By evaluating the physical properties of the fluids at the average film temperature, the Grashof and Prandtl numbers were determined at transition.

For water the initial instability occurred at a Grashof number of 5 or 6 x 10^8 and a Grashof-Prandtl number product of 2 or 3 x 10^9. For ethylene glycol the initial instability occurred at Grashof numbers from 3 to 6 x 10^7 and Grashof-Prandtl numbers of 1.3 to 5.7 x 10^9.

The results showed that the transition from laminar to turbulent flow is not a function of the Grashof number alone. However, no function of the Grashof and Prandtl numbers was found whereby the point of initial instability could be exactly correlated. As an approximation, the initial instability may be said to occur at a Grashof-Prandtl number product of 3 x 10^9.

RAO, N. N., "The Semi-Diurnal Lunar Variations of Ionospheric Layers," M.S. in Electrical Engineering, 1960.

An up-to-date review of the ionospheric "dynamo theory" of terrestrial magnetic variations is presented. Experimental evidence is collected in support of the location of the dynamo region at a height of 100 - 110 km. From the revised dynamo theory of Baker and Martyn and the ionospheric current systems deduced by Chapman and Bartels from the observed lunar daily magnetic variation L, the vertical ionization-drift velocities due to the semi-diurnal lunar tide have

(Continued on page 30)

Notes and Comments

ENGINEERS IN THE NEWS

M. M. David, Associate Professor of Chemical Engineering, was the co-author with H. Glaze, Jr., former Graduate Student, and M. G. Rao, Research Assistant, of papers presented January 11, at the Golden Jubilee Symposium, Indian Institute of Science, Bangalore, India. Professor David and A. F. Kiere, former student in Chemical Engineering, co-authored a paper given on December 28 at the Northwest Scientific Association in Spokane.

R. H. Bogan, Associate Professor of Civil Engineering, has received a new grant of $15,000 from the Aero-Space Division of the Boeing Airplane Company. The grant is to be used to continue the experimental investigation of the activated sludge process as a means of sustenance for men during space flight, a study described in the January *Trend*.

R. N. Kusian, Director of the Environmental Research Laboratory, is leaving the University to take over a position in the Hazards Control Unit of the Lawrence Radiation Laboratory, University of California, Livermore, California.

R. G. Hennes, Professor of Civil Engineering, has been assigned the task of setting up a graduate program in soil mechanics at the Bengal College of Engineering, Calcutta, India. The work is under the jurisdiction of the International Cooperation Administration. Professor Hennes will be in India for a year, beginning in June.

E. M. Horwood, Associate Professor of Civil Engineering, presented papers to sections of the Highway Research Board on January 11 and 13 in Washington, D. C.

J. I. Mueller, Professor of Ceramic Engineering, attended the annual meeting of the American Ceramic Society in Philadelphia during the last week in April. Professor Mueller is vice-president of the Society.

James W. Souther, Associate Professor of Humanistic-Social Studies, has been elected Chairman of the English Division of ASEE.

A University press publication, *Men and Moments in the History of Science,* edited by Herbert M. Evans, is a collection of talks by distinguished California scientists delivered at meetings of a dinner club devoted to the history of Science.

The University is to have a new computer building, which is to be completed in the summer of 1961.

NEW PROJECTS

Project No. 271. Development of a Research Demonstration Flume for Open Channel Flow. Supervisor: E. P. Richey, Associate Professor of Civil Engineering; Research Assistant: J. F. Roth, Jr.

Project No. 272. Influence of Nuclear Radiation on Boiling Heat Transfer. Supervisor: P. J. Waibler, Associate Professor of Mechanical Engineering; Research Assistant: Meldon H. Merrill.

Project No. 273. Single-Particle Rate Studies in Ion Exchange. Supervisor: M. M. David, Associate Professor of Chemical Engineering; Research Assistant: Norman L. Eatough.

Project No. 274. SO_2-H_2O-NH_3 Equilibria. Supervisors: J. L. McCarthy, Professor of Chemical Engineering, and L. N. Johanson, Associate Professor of Chemical Engineering; Research Assistant: William D. Scott.

Project No. 275. Interfacial Resistance in Liquid Systems. Supervisor: W. J. Heideger, Assistant Professor of Chemical Engineering; Research Assistant: A. Vasudev.

Project No. 276. Reactivity Effects of Fuel Burnup in Nuclear Reactors. Supervisor: D. E. McFeron, Professor of Mechanical Engineering; Research Assistant: C. W. Savery.

Project No. 277. Control-Rod Studies for UWTR. Supervisor: D. E. McFeron, Professor of Mechanical Engineering; Research Assistant: J. H. Smith.

Project No. 278. Investigation of Stresses in Piles and in Surrounding Soil when Piles Are Laterally Loaded. Supervisor: M. I. Ekse, Professor of Civil Engineering; Research Assistant: J. J. Furney.

Project No. 279. Noise Characteristics of Parametric Amplifiers. Supervisor: J. L. Bjorkstam, Assistant Professor of Electrical Engineering; Research Assistant: R. E. Oettel.

Project No. 280. Construction and Electrical Properties of Tunnel Diodes. Supervisor: J. L. Bjorkstam, Assistant Professor of Electrical Engineering; Research Assistant: C. Sienkiewicz.

Project No. 281. Self-Adjusting Control Systems. Supervisor: R. N. Clark, Associate Professor of Electrical Engineering; Research Assistant: P. C. Wheeler.

Project No. 282. Afterburner-Type Smog Eliminator. Supervisor: J. C. Firey, Associate Professor of Mechanical Engineering; Research Assistant: D. Ryder.

Project No. 283. On the Accuracy of the Birefringent Coating Method of Experimental Stress Analysis. Supervisor: A. S. Kobayashi, Assistant Professor of Mechanical Engineering; Research Assistant: C. Larson. This project has been discontinued.

Project No. 284. Uses of a Digital Computer in Engineering Design. Supervisor: P. L. Balise, Associate Professor of Mechanical Engineering; Research Assistant: R. F. Poultney.

Project No. 285. Measurement of Noise in a Tunnel Diode. Supervisor: K. Shimada, Assistant Professor of Electrical Engineering; Research Assistant: W. H. Eckton, Jr.

Project No. 286. Stress Analysis of Truncated Cones. Supervisor: E. H. Dill, Associate Professor of Aeronautical Engineering; Research Assistant: P. J. Chen.

Project No. 287. Kinetic Studies of the Nitric Acid-Nitrous Acid-Water System. Supervisor: A. L. Babb, Associate Professor of Chemical Engineering; Research Assistant: D. M. Waldorf.

Project No. 288. A Study of the Factors Controlling Anaerobic Reaction Rates. Supervisor: R. H. Bogan, Associate Professor of Civil Engineering; Research Assistant: K. K. Chin.

LUNAR TIDAL VARIATIONS

(Continued from page 22)

16. SINGER, S. F., *et al*, "Dynamo Currents and Conductivities in the Earth's Upper Atmosphere," *Nature*, Vol. 170, 1952, p. 1093.
17. CHAPMAN, S., and BARTELS, J., *Geomagnetism*, (Oxford University Press), 1940.
18. MARTYN, D. F., "The Normal F Region of the Ionosphere," *Proc., I.R.E.*, Vol. 47, 1959, p. 147.
19. RATCLIFFE, J. A., *et al*, "The Rates of Production and Loss of Electrons in the F Region of the Ionosphere," *Phil Trans. Roy. Soc.*, A, Vol. 248, 1956, p. 621.
20. MITRA, S. K., *The Upper Atmosphere*, (The Asiatic Society, Calcutta), 1952, p. 290.
21. APPLETON, E. V., and LYON, A. J., "Ionospheric Layer Formation under Quasi-Stationary Conditions," *The Physics of the Ionosphere*, (The Physical Society, London), 1955, p. 20.
22. APPLETON, E. V., "The Normal E Region of the Ionosphere," *Proc., I.R.E.*, Vol. 47, 1959, p. 155.

THE SEMI-DIURNAL LUNAR VARIATIONS

(Continued from page 28)

been calculated by the author for different ionospheric heights. It is found that the vertical drift velocity has a large height gradient at E-region heights, contrary to earlier assumptions.

The effect of this vertical drift velocity on both the daytime and nocturnal ionization of the E and F_2 layers is investigated. The theoretical results obtained by the author are then compared with the available experimental data for the harmonic coefficients of the semi-diurnal lunar oscillations of the ionospheric layers. The theoretical results for the F_2-layer variations seem to be in good agreement with the experimental results, whereas in the case of E-layer variations the comparison indicates a general disagreement between the two. An attempt is made to explain this disagreement.

STRALEY, R. L., "The Use of Metallic Thermocouples as Heat Engines," M.S. in Mechanical Engineering, 1960.

The concern of this thesis is the theoretical analysis of the metallic thermocouple as a heat engine and an experimental analysis of the effect of surface-diffused impurities.

A review of the fundamental theory of the thermoelectric effect and a thermodynamic analysis of the metallic thermocouple are presented to determine their parameters.

The variation of the thermoelectric parameters with the composition of binary alloys is presented. The general effect of a radiation field on the thermoelectric properties of a metal is discussed, and the effect of "thermal" neutrons upon copper is analyzed.

An experimental analysis is made of the variation of the thermoelectric properties of copper resulting from the diffusion of nickel radially into a test rod. These results are compared with a theoretical analysis.

Why not a two-way street? The question of how big a place the humanities should occupy in engineering education has frequently been investigated in *Trend* editorials; and the topic is still wide open for discussion. An angle of the subject examined recently in *Saturday Review* is sometimes neglected. In an article predicting the directions technology may take in this decade, Roger Burlingame says: "If we get time to think, we can do something with education. There is much talk about introducing studies of the humanities into engineering curricula and there are occasional instances of success. But how about the converse of this program? How about getting more science and technology into the teaching of the liberal arts? We should begin this at the elementary level. Surround the child with models of what he must live with; show him how each thing evolved from something else; show him what is behind every button he pushes, every picture on the screen, how 150 horses got under the hood of Daddy's car. The man or woman emerging from this kind of instruction will no longer be at the mercy of a managerial priesthood which is coming to possess all the 'knowhow.' Such an educational equipment, coupled with natural—not synthetic—human desire, will enable us to lead the technology we now follow." From Roger Burlingame, "The Sixties: Coming up in Technology," *Saturday Review*, Vol. XLIII, No. 2, Jan. 9, 1960.

A NEUTRON ABSORPTIOMETER FOR THE ON-STREAM ANALYSIS OF BORON

(Continued from page 3)

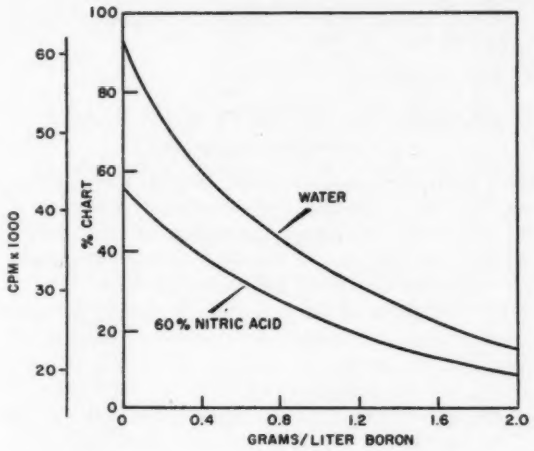

FIG. 3. CALIBRATION CURVE

measuring annulus of 1⅜ in. had adequate sensitivity within the range of zero to 2 g per liter of boron. The calibration curve of the completed unit is shown in Fig. 3.

Seal Pot. The function of the seal pot is to provide a liquid pressure seal between the process and operating gallery. The seal pot will always contain sufficient solution to provide 5 ft of water head in event of a positive pressure in the process. The process vessel is equipped with a pressure relief for 2 ft of water. Flow tests of the seal pot and sensing cell indicated the unit will pass 150 gal per minute with a full make-up tank.

Instrumentation

The electronic instrumentation selected for thermal neutron measurements is standard counting instruments that have good reliability and accuracy. A block diagram of the instrumentation is shown in Fig. 4. The BF_3 neutron detector tube is an ionization chamber filled with enriched BF_3 gas. If a neutron penetrates the counting portion of the tube and is captured by a nucleus of the gaseous boron-10, an alpha particle is emitted and the boron-10 is converted to Lithium-7:

$$_5B^{10}+_0n^1\rightarrow_3L^7+_2He^4+Q\,.$$

The alpha particle creates an ionization, and a voltage pulse is produced that may be counted by suitable electronic circuitry.

Immediately above the BF_3 tube is located a linear

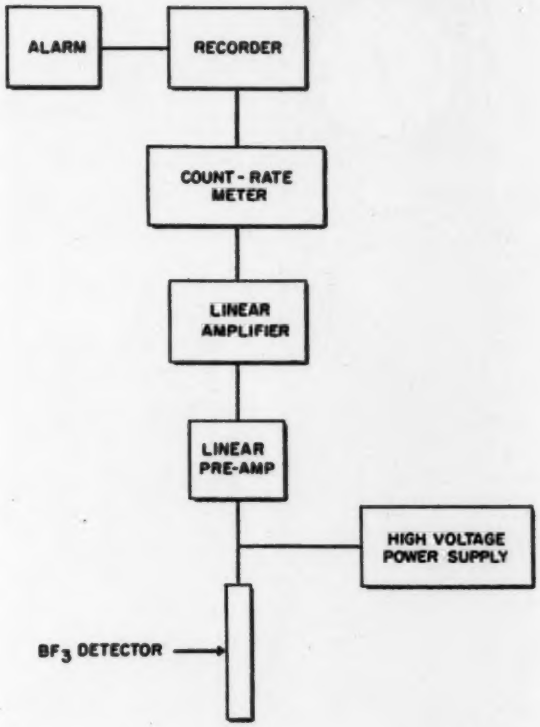

FIG. 4. BLOCK DIAGRAM OF INSTRUMENTATION

preamplifier. It is as near as possible to the tube in order to minimize loss of pulse height resulting from the voltage pulse from the tube being attenuated by the capacitance and low impedance of the cable to the preamplifier. The preamplifier gives a voltage gain of approximately 10; it has a low output impedance that permits counting instrumentation to be located several hundred feet away from the basic sensing unit.

A well-stablized high-voltage power supply provides approximately 1500 v, dc, to operate the BF_3 tube in its "plateau" region.

A linear amplifier receives the voltage pulses from the preamplifier and amplifies them to a usable level. The pulses are then fed to the count-rate meter, which measures the instantaneous rate of counting and produces a 0 to 50 mv signal proportional to the rate. A circular chart recorder is used to record the counting rate. An adjustable alarm circuit is located inside the recorder to operate the alarm lights when the

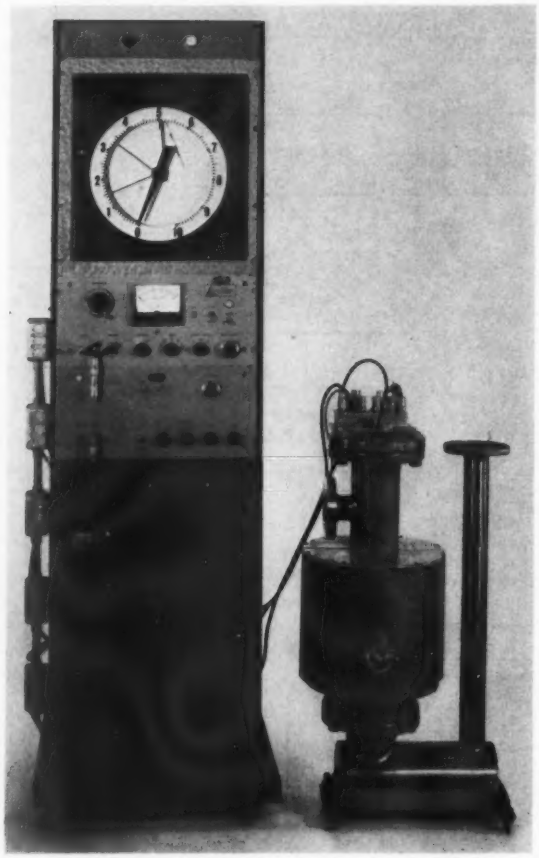

FIG. 5. THE NEUTRON ABSORPTIOMETER

counting rate of the instrument exceeds a predetermined value. The time constant of the instrumentation totals 5 sec.

Conclusion

A neutron absorptiometer developed for the on-stream analysis of boron in the range of 0 to 2 g per liter is shown in Fig. 5. The unit has been calibrated to measure boron in solutions of water, 60% nitric acid, 50% sodium hydroxide, and 38% sodium nitrate. The monitor could be used to measure the concentration of any solute with a large thermal neutron cross section compared to the solvent. The construction materials must be such that they present a low neutron absorption cross section immediately surrounding the neutron source and monitored solution. Future applications might use lucite, polyethylene, aluminum, zirconium, and stainless steel as construction materials.

The monitor and instrumentation have been installed in the plant and are presently being evaluated.

REFERENCES

1. R. W. STROMATT, *Literature-Review on Boron Analysis,* Hanford AEC Report HW-58184, Oct. 24, 1958.
2. D. D. DeFORD and R. S. BRAMAN, *A Study of Neutron Absorptiometry and Its Application to the Determination of Boron,* Callery Chemical Co. Report CCC-1024-TR-243, May 17, 1957.

WATER DISINFECTION AT A BEACH

(Continued from page 10)

their apprehension about water quality. For this reason the report recommends continued operation of the chlorination facility until public confidence in our bathing beaches can be restored through the many sewerage improvements now being planned.

The operation of the chlorination facility must be in the hands of a responsible person employed full time for the work. This person can perform other duties, but his primary duty must be this facility. If operation is not continuous and effective, it is a waste of money, and it will not engender confidence from the public.

Daily records of the operation should be kept as a protection to the City and for the valuable data they provide in increasing our general knowledge of such installations.

Arrangements should be made with the Seattle-King County Health Department for collection and analysis of weekly bacteriological samples from the West and East Beaches and from the Lake itself outside the swimming areas and away from the shoreline. These samples can be collected by the facility operator.

An automatic control should be placed in the chlorination system, a control that will shut off the chlorinator and the pump if the pump loses its suction and ceases to deliver water.

For an effective bacterial kill, the chlorine residual in the water where bathers and swimmers congregate should be maintained between 0.4 and 0.6 ppm. Bacteriological tests will aid in setting the desired chlorine residual. Possibly a lower chlorine residual may be maintained in the summer of 1960.

REFERENCES

1. R. O. SYLVESTER, *Report on Interim Treatment for Green Lake,* Report to Seattle Park Board, April 14, 1959.
2. R. O. SYLVESTER and G. C. ANDERSON, *An Engineering and Ecological Study for the Rehabilitation of Green Lake,* Report to Seattle Park Board, February 6, 1960.
3. R. T. RAVENHOLT, *Proposed Investigation of Beach Waters and Health,* Seattle-King County Health Department, February, 1959.
4. *Water Quality Objectives,* Pollution Control Council, Pacific Northwest Area, 1952.
5. *Design, Equipment and Operation of Swimming Pools and Other Public Bathing Places,* American Public Health Association Bulletin, 1949.

PUBLICATIONS

of the

ENGINEERING EXPERIMENT STATION

UNIVERSITY OF WASHINGTON

Requests for copies of publications should be addressed to the Director, Engineering Experiment Station, University of Washington, Seattle 5.

BULLETINS

48. The Influence of Pipe Thickness on Re-Entrant Intake Losses. Charles William Harris. 33 pp. 1928.
54. Elimination of Hydraulic Eddy Current Loss at Intake. Charles William Harris. 30 pp. 1930.
55. Vacuum-Tube Control for Electric Wind-Tunnel Balances. Fred S. Eastman. 20 pp. 1931.
56. Constant Flow Characteristic of the Plane Orifice in Proximity to Side Walls. Charles William Harris. 18 pp. 1931..
58. Preliminary Tests of Thirteen Washington Coals in a Powdered Coal Boiler Plant at the University of Washington. George Samuel Wilson, Harry Fagan Yancey, and Joseph Daniels. 27 pp. 1931.
60. An Electromagnetic Balance for Force Measurement of Current Control. Fred Scoville Eastman. 29 pp. 1932.
61. Hydraulic Flow Characteristics of a Square-Edged Intake. Charles William Harris. 21 pp. 1932.
67. The Doherty Washer Cooler, Sybren Ruurd Tymstra. 61 pp. 1932.
72. The Derivation of the Mean Temperature Difference Between a Saturated Gas and a Cooling Liquid, and also the Derivation of the Mean Velocity of Such Gas. Sybren Ruurd Tymstra. 19 pp. 1933.
74. The Deformation of Hard Grade Reinforcing Steel During and After Construction in a Reinforced Concrete Building. Sergius Ivan Sergev. 33 pp. 1933.
75. The Water Tube Gas Condenser. Sybren Ruurd Tymstra. 24 pp. 1934.
76. Kaolin and China Clay in the Northwest. Hewitt Wilson. 184 pp. 1934. (Loan only.)
77. A Study of Fundamental Relations of the Mathematical Theory of Elasticity. Arthur Melvin Winslow. 25 pp. 1934. (Loan only.)
81. Influence of Two Secondary Factors in Weir Measurement. Charles William Harris. 16 pp. 1935.
85. Discharge of Three Commercial Cippoletti Weirs. Robert Bowman Van Horn. 32 pp. 1935.
87. Open Water Testing of Ship Models. Thomas McKie Rowlands. 20 pp. 1935.
88. The Properties of Quartz Sands Washed from Kaolins of the Pacific Northwest. Hewitt Wilson and Frank Joseph Zvanut. 42 pp. 1936.
91. The Analysis and Control of Landslides. Robert Graham Hennes. 57 pp. 1936. (Loan only.)
92. Moment Equations. A Method of Analysis for Continuous Beams and Rigid Frames. Alfred Jensen. 88 pp. 1937.
94. Evaporation and Surface Cooling. George Samuel Wilson and William Lyle Dudley. 18 pp. 1937.
98. Geology and Its Relation to the Occurrence of Oil in Washington. Charles Edwin Weaver. 16 pp. 1938.
100. Modernization of a Transit System. Factors that Determine the Choice of a Vehicle. George Lisle Hoard. 36 pp. 1940.
101. Buckling Criteria and Design of Two-Story Columns. Sergius I. Sergev. 48 pp. 1940.
102. An Investigation of Prestressed Stays. T. M. Rowlands and F. C. Smith. 36 pp. 1941.
103. Bismuth Bridge Magnetic Flux Meter. George Sherman Smith. 48 pp. 1940.
104. The Telechronometer, Telephone Service Measurement in Units of Time. Lyall Baker Cochran. 68 pp. 1941.
106. The Shearing Strength of Cement Mortar. Frederick C. Smith and Robert Q. Brown. 32 pp. 1941. (Loan only.)
108. Silica Sands of Washington. Hewitt Wilson, Kenneth C. Skinner, and Albert H. Couch. 76 pp. 1942.
109. The Number of Teeth in Contact as a Vibration Factor in Involute Cut Gears. Sybren Ruurd Tymstra. 16 pp. 1942.
110. Solutions for Torsional Vibration Frequencies by Energy Method. Arthur Melvin Winslow. 22 pp. 1943.
111. Stabilized Earth Blocks for Protective Construction. Robert G. Hennes. 24 pp. 1943.
112. Hydraulic Models. Charles W. Harris. 17 pp. 1944.
113. The Theoretical Behavior and Design of Initially Curved Struts Under an Intermediate Concentric Axial Load. Sergius I. Sergev. 32 pp. 1945.
114. The Effect of Shearing Forces on the Deflection and Strength of Beams. Sergius I. Sergev. 20 pp. 1947.
116. Aerodynamic Stability of Suspension Bridges with Special Reference to the Tacoma Narrows Bridge. Part I. Investigations Prior to October, 1941. F. B. Farquharson. 103 pp. 1949. (Loan only.)
116. Aerodynamic Stability of Suspension Bridges with Special Reference to the Tacoma Narrows Bridge. Part II, Mathematical Analyses. F. C. Smith and G. S. Vincent. 63 pp. 1950.
116. Aerodynamic Stability of Suspension Bridges with Special Reference to the Tacoma Narrows Bridge. Part III, The Investigation of Models of the Original Tacoma Narrows Bridge Under the Action of Wind. F. B. Farquharson. 125 pp. 1952.
116. Aerodynamic Stability of Suspension Bridges with Special Reference to the Tacoma Narrows Bridge. Part IV. The Investigation of Models of the New Tacoma Narrows Bridge Under the Action of Wind. F. B. Farquharson. 104 pp. 1954.
116. Aerodynamic Stability of Suspension Bridges with Special Reference to the Tacoma Narrows Bridge. Part V, Extended Studies: Logarithmic Decrement, Field Damping, Prototype Predictions, Four Other Bridges. G. S. Vincent. 104 pp. 1954.
118. Investigations in Aeronautics from the Department of Aeronautical Engineering. Edited by R. M. Rosenberg. 120 pp. 1951.
119. The Extremum Principles of the Mathematical Theory of Elasticity and Their Use in Stress Analysis. (The Walker-Ames lectures of the Spring Quarter, 1950.) W. Prager (Brown University). 30 pp. 1951.

REPORTS

2. Iron and Steel Manufacture in Washington, Oregon, California, and Utah. Joseph Daniels. 69 pp. 1929. (Loan only.)
3. Coal in Washington. Joseph Daniels. 17 pp. 1934. (Loan only.)
4. Water Resources of Washington. Richard Gaines Tyler. 61 pp. 1938 (Loan only.)
7. A Natural Uranium-Graphite Subcritical Reactor System for Education and Research. Part I. Description and Experimental Measurements. A. L. Babb, L. Grimsrud, W. E. Wilson. Part II. IBM 650 Computer Programs for Effective Size, Diffusion Length, and Material Buckling Calculations. A. L. Babb, L. Grimsrud, S. Tashiro. 33 pp. 1959.

TECHNICAL NOTES

3. The Theory of Fractional Parts Developed for Structural Beam-Column Members Preceded by an Elementary Discussion of Simple Beam and Column Design. Sybren Ruurd Tymstra. 32 pp. 1934. (Loan only.)
4. Gaging Chart for Horizontal Cylindrical Tanks with Flat Heads or with Convex Heads. Sybren Ruurd Tymstra. 4 pp. 1944.
5. Gaging Chart for Cylindrical Tanks with Different Types of Heads. Sybren Ruurd Tymstra. 7 pp. 1945.

TREND REPRINTS AVAILABLE

T3. A New Critical Phase of the Lake Washington Pollution Problem. R. O. Sylvester, W. Thomas Edmondson, R. H. Bogan. 7pp. 1956.

T8. Who's Going to Teach Them and How. Editorial Study. 2 pp. 1957.

T9. A Model Study of Some Fish Facilities for the Proposed Mayfield Dam. Part I: The Skimmer. E. P. Richey and H. H. Chenoweth. 8 pp. 1957.

T12. Professional Ethics and Engineering Education. A Arthur Hemenway. 1 p. 1958.